Superconvergence for Diffusion Reaction Equation by Weak Galerkin Finite Element Methods

by

Yu Zhang

(Under the Direction of Lin Mu)

Abstract

In this thesis, we apply stabilizer free weak Galerkin finite element methods using linear basis functions to achieve superconvergence of order four for L^2 norm and superconvergence of order three for energy norm for Diffusion-Reaction equations. We carefully discuss the scheme, and provided numerical experiment results as validation for the desired convergence rate.

Index words: [Superconvergence, finite element methods, weak Galerkin, weak gradient]

Superconvergence for Diffusion Reaction Equation by Weak Galerkin Finite Element Methods

by

Yu Zhang

B.A., University of Minnesota, 2019

A Thesis Submitted to the Graduate Faculty of the
University of Georgia in Partial Fulfillment of the Requirements for the Degree.

Master of Arts

Athens, Georgia

2022

Superconvergence for Diffusion Reaction Equation by Weak Galerkin Finite Element Methods

by

Yu Zhang

Major Professor: Lin Mu

Committee: Ming-Jun Lai
Weiwei Hu

Electronic Version Approved:

Ron Walcott
Vice Provost for Graduate Education and Dean of the Graduate School
The University of Georgia
August 2022

Acknowledgments

I would like to express the deepest appreciation to my advisor Dr. Lin Mu, whom is not only an outstanding scholar but also a wonderful, selfless, and supportive mentor. Dr. Mu's knowledge and dedication to research and teaching inspired me to be a better student. Without her guidance and persistent help, this thesis would not have been possible. Dr. Mu's journey in life has also taught me so many valuable lessons in my personal life.

I'm very grateful for all the help Dr. Seulip Lee has provided me with. I'm thankful for all of the time he spent preparing our meeting notes and carefully explaining every details. I'm thankful for his patience and encouragement. I'm grateful for his generosity when it comes to sharing his knowledge and path in Mathematics.

I would like to thank Dr. Ming-Jun Lai, and Dr. Weiwei Hu for serving as my committee members and share their insights and expertise on my research. I would like say thank you to Dr. Qing Zhang for suggesting reaching out to Dr. Mu for research ideas in the first place. In addition, a thank you to Dr. Giorgis Petridis, for his support and encouragement when I was down.

I'm really fortunate to have became friends with Nicole Song, Lou Han, Zack Garza, Peter Woolfitt, and Zhaiming Shen. They have supported and helped me when needed. They have also made these three years of my life more enjoyable.

Table of Contents

Chapter 1

Introduction

The reaction diffusion equations are widely used in modeling population dynamics, chemical reactions, and certain physics phenomena, [7]. The general form of diffusion-reaction equations is

$$\frac{\partial u}{\partial t} = d\Delta u + f(u),$$

where d is a positive constant. The left hand side term stands for time dependent variables, whereas $d\Delta u$ acts as the diffusion term, and $f(u)$ describes the rate of formation of the components. In chemistry, these equations represent how the rate of chemical components' diffusion interact with the rate of their production.

There are numerous numerical methods for solving partial differential equations, such as finite difference methods (FDMs), finite element methods (FEMs), and finite volume methods (FVMs). They all have their own advantages and shortcomings. FDMs approximate the derivatives by finite differences. It's relatively easy to implement if the domain of the problem is rectangular, however, this method is not efficient when handling curved domains [10]. FVMs approximate PDE solutions in forms of algebraic equations that satisfy certain conservation laws. FVMs can be used to approximate solutions over a complicated domain, however, the global converging order can not be easily improved by refining the mesh [4]. FEMs discretize large domains into smaller sub-domains, then approximate the solutions on each sub-domains by reducing associated errors, eventually, put all approximated solutions together using piece-wise functions. There are many benefits of FEMs including but not limited to handling complex domains and ease of adjusting the degree of the approximated solutions. However, comparing to FDMs and FVMs, FEMs are harder to implement due to the systems' complexity [3]. Approximating PDE solutions with splines is also a well studied subject. [5] by Gutierrez, Lai, and Slavov discussed the solution for diffusion-reaction equations using bivariate splines.

Weak Galerkin finite element methods were first introduced in [12] by Wang and Ye for second-order elliptic problems. Comparing to the standard Galerkin finite element method which requires the approximating functions to be continuous polynomials, weak Galerkin finite element methods define weak

gradients to allow the approximation solutions to be discontinuous. Allowing discontinuous approximation has two advantages [14]:

1. it's easy to construct high order elements;
2. it's easy to work on general meshes.

Yet, discontinuous approximation may run into issues with stability, thus often requires stabilizing terms to achieve stability and convergence, which add to the complexity of the formulation. By defining some particular weak gradients, [14] introduced stabilizer free weak Galerkin finite element method (SFWG) for the first time. The optimal way of defining the weak gradient is established in [11].

Achieving a high convergence rate has always been an important goal of numerical solutions for PDEs. For example, the standard finite element method for solving Poisson's equation with linear equation as bases have first-order convergence [1]. A method is considered to be superconvergent if the convergence rate exceeds general expectation.

In this thesis, we will apply SFWG to a diffusion-reaction equation and prove that it achieves superconvergence order of order 3 for energy norm and order 4 for L^2 norm. Furthermore, we conduct numerical experiments to validate the theoretical results.

The thesis is structured as follows: In chapter 2, we will define the finite element scheme in one dimension, conduct error analysis and numerical experiments. We extend the result to two dimensions in chapter 3.

We consider the following reaction diffusion equation in this thesis,

$$-\Delta u + cu = f, \text{ in } \Omega \tag{1.1}$$

$$u = 0, \text{ on } \partial\Omega. \tag{1.2}$$

where Ω is $[a, b]$ in one dimension case and is $[a, b] \times [a, b]$ in two dimension case, and c is a positive constant.

Let D be any domain in one or two dimension. We adopt the standard notation for Sobolev space $H^s(D)$ and their associated inner products $(\cdot, \cdot)_{s,D}$, norms $\| \cdot \|_{s,D}$. When $s = 0$, the space $H^s(D)$ coincides with $L^2(D)$, for which the norm and the inner product are denoted by $\| \cdot \|_D$ and $(\cdot, \cdot)_D$, respectively. When $D = \Omega$, we drop the subscript D in the norm and inner product notation. In one dimension, we have:

$$\|u\|_{0,D} = \|u\|_D = \sqrt{(u, u)_D} = \left(\int_D |u|^2 dx \right)^{\frac{1}{2}},$$

$$\|u\|_{\partial D} = (u(x_{i+1})^2 + u(x_i)^2)^{\frac{1}{2}}.$$

In two dimension, we have:

$$\|u\|_D = \sqrt{(u, u)_D} = \left(\int_D |u|^2 dx \right)^{\frac{1}{2}},$$

$$\|u\|_{e \subseteq \partial D} = (\int_e |u|^2 dx)^{\frac{1}{2}}.$$

Let $H_0^1(\Omega)$ denote the closure in $H^1(\Omega)$ of the space of infinitely differentiable compactly supported functions, where

$$H^1(\Omega) = \{f \in L^2(\Omega); \partial_x f \in L^2(\Omega), \partial_y f \in L^2(\Omega)\}.$$

Note that $H_0^1(\Omega) \subseteq H^0(\Omega)$.

Chapter 2

Superconvergent weak Galerkin finite element methods for one dimensional reaction-diffusion equation

2.1 Preliminaries and Notations

In this section, we define the mesh, the stabilizer free weak Galerkin finite element space, and the weak gradient.

Let $\Omega = \bigcup_{i=1}^{N} I_i$ with $I_i = [x_{i-1}, x_i]$ and $\mathcal{T}_h = \{I_i | i = 1, \cdots, N\}$, where the mesh size is denoted as $h = \max |I_i|$. For a given integer $k \geq 1$, let V_h be the weak Galerkin finite element space associated with $\mathcal{T}_h$ defined as follows:

$$V_h = \{v = \{v_0, v_b\} : v_0|_I \in P_k(I), v_b|_x \in P_0(x), x \subset \partial I, I \in \mathcal{T}_h, v_b|_{\partial\Omega} = 0\} \tag{2.1}$$

In one dimensional case, v_b takes a single value on x_i for $i = 1, \cdots, N$.

Definition 2.1.1. *For $v \in V_h$, a weak derivative $D_w v$ is a piecewise polynomial such that on each I_i, $D_w v \in P_{k+1}(I_i)$ satisfies*

$$(D_w v, q)_{I_i} = -(v_0, Dq)_{I_i} + \langle v_b, q\rangle_{\partial I_i} \quad \forall q \in P_{k+1(I_i)}, \tag{2.2}$$

where $\langle v_b, q\rangle_{\partial I_i} = v_b(x_i)q(x_i) - v_b(x_{i-1})q(x_{i-1})$, and Dq is the derivative of q.

For example, in the case where $k = 1$, the weak derivative of v on interval I is defined to be quadratic polynomial, such that for all degree 2 polynomial q on I we have

$$(D_w v, q)_I = -(v_0, Dq)_I + v_b(x_i)q(x_i) - v_b(x_{i-1})q(x_{i-1}).$$

For simplicity, we adopt the following notations,

$$(v,w)_{\mathcal{T}_h} = \sum_{i=1}^{N}(v,w)_{I_i} = \sum_{i=1}^{N}\int_{I_i} uwdx, \tag{2.3}$$

$$\langle v,w\rangle_{\partial\mathcal{T}_h} = \sum_{i=1}^{N}\langle v,w\rangle_{\partial I_i} = \sum_{I=1}^{N}\left(v(x_i)w(x_i) - v(x_{i-1})w(x_{i-1})\right). \tag{2.4}$$

Algorithm 2.1.1. *A SFWG finite element method for* (1.1) − (1.2) *seeks* $u_h \in V_h$ *such that*

$$(D_w u_h, D_w v) + c(u_0,v_0) = (f,v_0), \forall v \in V_h. \tag{2.5}$$

For any $v \in V_h$, we define two semi-norms,

$$|||v|||^2 = (D_w v, D_w v) + c\|v_0\|^2, \tag{2.6}$$

$$\|v\|_{1,h}^2 = \sum_{I\in\mathcal{T}_h}\left(\|Dv_0\|_I^2 + h_I^{-1}\|v_0 - v_b\|_{\partial I}^2\right) + c\|v_0\|^2. \tag{2.7}$$

2.2 Well-posedness of the scheme

Theorem 2.2.1. *Algorithm 2.1.1 will give an unique solution.*

Proof. By the definition of the energy norm (2.6), we can see that it is indeed an norm, i.e. $|||v||| = 0$, if and only if $v = 0$. Thus, it guarantees the uniqueness of the solution. Therefor, the SFWG method is well posed. □

Lemma 2.2.1. *There exist a positive constant* C_1 *independent of h, such that for any* $v \in V_h$*, we have*

$$C_1\|v\|_{1,h} \le |||v||| \tag{2.8}$$

Proof. Choose $q \in P_{k+1}(I_i)$ on each I_i such that

$$q(x_{i-1}) = h^{-1}\left(-v_b(x_{i-1}) + v_0(x_{i-1})\right),$$

$$q(x_i) = h^{-1}\left(v_b(x_{i-1}) - v_0(x_{i-1})\right),$$

$$(q,p_{k-1})_I = (Dv_0,p_{k-1})_I + c(v_0,v_0)_I,\ \forall p_{k-1} \in P_{k-1}(I_i).$$

Since $q \in P_{k+1}(I_i)$, it will have $k+2$ coefficient and they can be determined by the above equations.

By the finite dimensional norm equivalence and the scaling argument,

$$\|q\| \le C\|v\|_{1,h}.$$

By (2.2), with above q, and Cauchy-Schwarz inequality, we get

$$\|v\|_{1,h}^2 = (D_w v, q) \le \|D_w v\|\|q\| \le |||v|||\|v\|_{1,h}.$$

□

2.3 Error Analysis

2.3.1 Error Equation

Let Π_j be the element-wise defined L^2 projection onto $P_j(I)$ for $I \in \mathcal{T}_h$ and $Q_h u = \{\Pi_k u, u\} \in V_h$.

Lemma 2.3.1. *Let $\phi \in H^1(\Omega), q \in P_{k+1}(I)$. Then on any $I \in \mathcal{T}_h$, we have*

$$(D_w(Q_h\phi), q) = (\Pi_{k+1}(D\phi), q). \tag{2.9}$$

Proof. Using the definition of weak derivative (2.2), definition of L^2 projection, integration by parts, and definition of L^2 project, we have that for any $q \in P_{k+1}(I)$

$$\begin{aligned}(D_w(Q_h\phi), q)_I &= -(\Pi_k\phi, Dq)_I + \langle \phi, q\rangle_{\partial I} \\ &= -(\phi, Dq)_I + \langle \phi, q\rangle_{\partial I} \\ &= (D\phi, q)_I \\ &= (\Pi_{k+1}(D\phi), q)_I,\end{aligned}$$

which implies Lemma 2.3.1.

□

Let $e_h = Q_hu - u_h = \{\Pi_k u - u_0, u - u_b\} \in V_h$. Then, the error equation for e_h is derived as follows.

Lemma 2.3.2. *For any $v = \{v_0, v_b\} \in V_h$, it holds*

$$(D_we_h, D_wv) + c(u - u_0, v_0) = l(u, v),$$

where

$$\ell(u, v) = \langle Du - \Pi_{k+1}Du, v_0 - v_b\rangle_{\partial\mathcal{T}_h}.$$

Proof. To begin with, we multiply the main equation (1.1) by a test function v_0 and use integration by parts to obtain

$$(f, v_0) = (-u'' + cu, v_0) = (Du, Dv_0)_{\mathcal{T}_h} - \langle Du, v_0\rangle_{\partial\mathcal{T}_h} + c(u, v_0).$$

Since Du is continuous at all the interior points in $\mathcal{T}_h$ and $v_b = 0$ at the boundary points, we have

$$\langle Du, v_b\rangle_{\partial\mathcal{T}_h} = 0,$$

which implies

$$(f, v_0) = (Du, Dv_0)_{\mathcal{T}_h} - \langle Du, v_0 - v_b\rangle_{\partial\mathcal{T}_h} + c(u, v_0).$$

Moreover, it follows from the L^2 projection and integration by parts that

$$(Du, Dv_0)_{\mathcal{T}_h} = (\Pi_{k+1}Du, Dv_0)_{\mathcal{T}_h} = -(D(\Pi_{k+1}Du), v_0)_{\mathcal{T}_h} + \langle \Pi_{k+1}Du, v_0\rangle_{\partial\mathcal{T}_h}.$$

In this case, we note that $Dv_0 \in P_{k-1}(I)$ for any $I \in \mathcal{T}_h$, which makes it possible to take the L^2 projection of Du. Thus, by the definition of the weak derivative $D_wv \in P_{k+1}(I)$ in (2.2) , we arrive at

$$\begin{aligned}(Du, Dv_0)_{\mathcal{T}_h} &= (\Pi_{k+1}Du, D_wv)_{\mathcal{T}_h} + \langle \Pi_{k+1}Du, v_0 - v_b\rangle_{\partial\mathcal{T}_h} \\ &= (D_w(Q_hu), D_wv)_{\mathcal{T}_h} + \langle \Pi_{k+1}Du, v_0 - v_b\rangle_{\partial\mathcal{T}_h}.\end{aligned}$$

Indeed, the second equality holds because $\Pi_{k+1}Du = D_w(Q_hu)$ with respect to any polynomial of $P_{k+1}(I)$ in Lemma 2.3.1. Therefore, we have an intermediate result,

$$(-u'' + cu, v_0) = (f, v_0) = (D_w(Q_hu), D_wv)_{\mathcal{T}_h} - \langle Du - \Pi_{k+1}Du, v_0 - v_b\rangle_{\partial\mathcal{T}_h} + c(u, v_0). \tag{2.10}$$

Finally, by subtracting (2.5) from this intermediate result, we obtain

$$0 = (D_we_h, D_wv)_{\mathcal{T}_h} - \ell(u, v) + c(u - u_0, v_0).$$

We conclude the proof by moving $l(u, v)$ to the other side of the above equation.

□

2.3.2 Error Estimate in Energy Norm

For any function $\phi \in H^1(I_i)$, with $I_i = [x_{i-1}, x_i]$, the following trace inequality holds true:

$$\|\phi\|_{\partial I_i} \leq C(h_{I_i}^{-1}\|\phi\|_{I_i}^2 + h_{I_i}\|D\phi\|_{I_i}^2).$$

Lemma 2.3.3. *For any $w \in H^{k+3}(\Omega)$ and $v = \{v_0, v_b\} \in V_h$, we have*

$$|l(w, v)| \leq Ch^{k+2}|w|_{k+3}|||v|||. \tag{2.11}$$

Proof. By Cauchy-Schwarz inequality, we have

$$\begin{aligned} |l(w,v)| &= \left| \sum_{I\in\mathcal{T}_h} \langle Dw - \Pi_{k+1}Dw, v_0 - v_b\rangle_{\partial I} \right| \\ &\leq \sum_{I\in\mathcal{T}_h} \left(\|Dw - \Pi_{k+1}Dw\|_{\partial I}\|v_0 - v_b\|_{\partial I} \right). \end{aligned}$$

Applying Cauchy-Schwarz inequality for series, and multiplying and dividing by h at the same time, we arrive at:

$$\sum_{I\in\mathcal{T}_h} \left(\|Dw - \Pi_{k+1}Dw\|_{\partial I}\|v_0 - v_b\|_{\partial I} \right) \leq \left(\sum_{I\in\mathcal{T}_h} h_I\|Dw - \Pi_{k+1}Dw\|_{\partial I}^2 \right)^{\frac{1}{2}} \left(\sum_{I\in\mathcal{T}_h} h_I^{-1}\|v_0 - v_b\|_{\partial I}^2 \right)^{\frac{1}{2}}.$$

Applying trace inequality to $\|Dw - \Pi_{k+1}Dw\|_{\partial I}^2$, we have

$$\left(\sum_{I\in\mathcal{T}_h} h_I\|Dw - \Pi_{k+1}Dw\|_{\partial I}^2 \right)^{\frac{1}{2}} \leq C \left(\sum_{I\in\mathcal{T}_h} h_I \left(h_I^{-1}\|Dw - \Pi_{k+1}Dw\|_I^2 + h_I\|D(Dw - \Pi_{k+1}Dw)\|_I^2 \right) \right)^{\frac{1}{2}}.$$

After simplifying and applying interpolation error, we arrive at:

$$\left(\sum_{I\in\mathcal{T}_h} h_I\|Dw - \Pi_{k+1}Dw\|_{\partial I}^2 \right)^{\frac{1}{2}} \leq C(h^{2k+4}|w|_{k+3}^2)^{\frac{1}{2}} = Ch^{k+2}|w|_{k+3}.$$

By (2.7) and (2.2.1), we have

$$\left(\sum_{I\in\mathcal{T}_h} h_I^{-1}\|v_0 - v_b\|_{\partial I}^2 \right)^{\frac{1}{2}} \leq \|v\|_{1,h} \leq C|||v|||.$$

Combining the above steps, we have proved the lemma. □

Theorem 2.3.1. *Let $u_h \in V_h$ be the SFWG finite element solution of* (2.5)*. There exists a constant C such that*

$$|||Q_h u - u_h||| \leq Ch^{k+2}|u|_{k+3}. \tag{2.12}$$

Proof. Recall $e_h = \{\Pi_k u - u_0, u - u_b\}$. Let $v = e_h$ in Lemma 2.3.2, we have

$$l(u, e_h) = (D_w e_h, D_w e_h) + c(u - u_0, \Pi_k u - u_0).$$

Since $\Pi_k u - u_0 \in P_k(I)$, we can take the L^2 projection of $u - u_0$, thus

$$|l(u, e_h)| = (D_w e_h, D_w e_h) + c(\Pi_k u - u_0, \Pi_k u - u_0) = |||e_h|||.$$

By Lemma 2.3.3 applied to $v = e_h$, we have

$$l(u, e_h) \leq Ch^{k+2}|u|_{k+3}|||e_h|||.$$

Thus,

$$|||e_h||| \leq Ch^{k+2}|u|_{k+3}.$$

□

2.3.3 Error Equation in L_2 norm

The considered dual problem seeks $\Phi \in H_0^1(\Omega) \cap H^2(\Omega)$ satisfying

$$-\Phi'' + c\Phi = e_0 \quad \text{in } \Omega. \tag{2.13}$$

Assume that the following H^2-regularity holds:

$$\|\Phi\|_2 \leq c||e_0||. \tag{2.14}$$

Theorem 2.3.2. *Let $u_h \in V_h$ be the SFWG finite element solutions of* (2.5)*. Assume that* (2.14) *holds true. Then there exists a constant C such that*

$$\|\Pi_k u - u_0\| \leq Ch^{k+3}|u|_{k+3}. \tag{2.15}$$

Proof. Testing (2.13) by e_0, we have

$$\|e_0\|^2 = (-\Phi'' + c\Phi, e_0).$$

By letting $u = \Phi$ and $v = e_h$ in (2.10), we have

$$\|e_0\|^2 = (D_w Q_h \Phi, D_w e_h) + c(\Phi, e_0) - l(\Phi, e_h).$$

By the definition of L^2 projection and Lemma 2.3.2,

$$\begin{aligned}(D_w Q_h \Phi, D_w e_h) + c(\Phi, e_0) &= (D_w Q_h \Phi, D_w e_h) + c(\Pi_k \Phi, e_0) \\ &= l(u, Q_h \Phi).\end{aligned}$$

By triangle inequality, we have

$$\begin{aligned}\|e_0\|^2 &= |l(u, Q_h\Phi) - l(\Phi, e_h)| \\ &\leq |l(u, Q_h\Phi)| + |l(\Phi, e_h)|.\end{aligned} \tag{2.16}$$

By Cauchy-Schwarz inequality and the trace inequality, we have

$$\begin{aligned}|l(u, Q_h\Phi)| &= \left| \sum_{I \in \mathcal{T}_h} \langle Du - \Pi_{k+1}, \Pi_k \Phi - \Phi \rangle_{\partial I} \right| \\ &\leq \sum_{I \in \mathcal{T}_h} \|Dw - \Pi_{k+1} Dw\|_{\partial I} \|\Pi_k \Phi - \Phi\|_{\partial I} \\ &\leq \left(\sum_{I \in \mathcal{T}_h} h_I \|Du - \Pi_{k+1} Du\|_{\partial I}^2 \right)^{\frac{1}{2}} \left(\sum_{I \in \mathcal{T}_h} h_I^{-1} \|\Pi_k \Phi - \Phi\|_{\partial I}^2 \right)^{\frac{1}{2}}.\end{aligned}$$

Applying trace inequality and using interpolation error on the first term, we have

$$\begin{aligned}
&\left(\sum_{I\in\mathcal{T}_h} h_I\|Du-\Pi_{k+1}Du\|_{\partial I}^2\right)^{\frac{1}{2}}\\
&\leq C\left(\sum_{I\in\mathcal{T}_h} h_I\left(h_I^{-1}\|Du-\Pi_{k+1}Du\|_I^2+h_I\|D(Du-\Pi_{k+1}Du)\|_I^2\right)\right)^{\frac{1}{2}}\\
&\leq C\left(\sum_{I\in\mathcal{T}_h} h_I\left(h_I^{-1}(h_I^{k+2}|u|_{k+3,I})^2+h_I(h_I^{k+1}|u|_{k+3,I})^2\right)\right)^{\frac{1}{2}}\\
&\leq Ch^{k+2}|u|_{k+3}.
\end{aligned}$$

Applying trace inequality to the second term, we have

$$\left(\sum_{I\in\mathcal{T}_h} h_I^{-1}\|\Pi_k\Phi-\Phi\|_{\partial I}^2\right)^{\frac{1}{2}}\leq C\left(\sum_{I\in\mathcal{T}_h} h_I^{-1}\left(h_I^{-1}\|\Pi_k\Phi-\Phi\|_I^2+h_I\|D(\Pi_k\Phi-\Phi)\|_I^2\right)\right)^{\frac{1}{2}}.$$

By interpolation error and the fact that $\Phi\in H_0^1(\Omega)$, we have

$$\|\Pi_k\Phi-\Phi\|_I^2\leq h_I^4\|\Phi\|_2^2$$

and

$$\|D(\Pi_k\Phi-\Phi)\|_I^2\leq h^2\|\Phi\|_2^2.$$

Combining the three inequalities above, we have

$$\left(\sum_{I\in\mathcal{T}_h} h_I^{-1}\|\Pi_k\Phi-\Phi\|_{\partial I}^2\right)^{\frac{1}{2}}\leq h\|\Phi\|_2.$$

Thus,

$$|l(u,Q_h\Phi)|\leq Ch^{k+3}\|\Phi\|_2. \tag{2.17}$$

By Lemma 2.3.3, we also have

$$|l(\Phi,e_h)|\leq Ch|\Phi|_2|||e_h|||.$$

By (2.15), we have

$$|l(\Phi,e_h)|\leq Ch^{k+3}|\Phi|_2|u|_{k+3}.$$

Since $|\Phi|_2\leq\|\Phi\|_2$, we have

$$|l(\Phi,e_h)|\leq Ch^{k+3}\|\Phi\|_2|u|_{k+3}.$$

Thus, by using (2.16) and (2.17),

$$\|e_0\|^2\leq Ch^{k+3}|u|_{k+3}\|\Phi\|_2.$$

Finally, by H^2-regularity,

$$\|e_0\|\leq Ch^{k+3}|u|_{k+3},$$

as desired. □

2.3.4 A Locally Lifted P_{k+2} Solution

As L^2 norm error of the SFWG solution with linear basis function is order one convergent, we lift the solution to a P_3 solution which achieves order four convergencen for the L^2 norm. In the general case,

elementwise we compute a solution $\hat{u}_h \in \Pi_{I\in\mathcal{T}_h} P_{k+2}(I)$ for

$$(D\hat{u}_h - D_w u_h, Dp) = 0, \ \forall p \in \Pi_{I\in\mathcal{T}_h} P_{k+2}(I)\backslash P_0(I), \tag{2.18}$$

$$(\hat{u}_h - u_h, p) = 0, \ \forall p \in \Pi_{I\in\mathcal{T}_h} P_0(I). \tag{2.19}$$

Remark 2.3.1. *The square linear system of equations* (2.18)-(2.19) *has a unique solution because when* $u_h = 0$, (2.18) *implies* $\|D\hat{u}_h\|^2 = 0$ *and* $\hat{u}_h$ *is a constant on each* I. *By* (2.19), *the constant is zero.*

Theorem 2.3.3. *Let* $u \in H_0^1(\Omega) \cap H^{k+3}$ *be the exact solution of* (1.1)-(1.2). *Let* $u_h \in V_h$ *be the SFWG finite element solution of* (2.5). *Let* $\hat{u}_h \in \Pi_{I\in\mathcal{T}_h} P_{k+2}$ *be locally lifted solution of* (2.18)-(2.19). *Then there exists a constant* C *such that*

$$\|u - \hat{u}_h\| \leq Ch^{k+3}|u|_{k+3}. \tag{2.20}$$

Proof. By (2.19),

$$\Pi_0 \hat{u}_h = \Pi_0 u_h.$$

We separate the error into two parts:

$$\|u - \hat{u}_h\| \leq \|\Pi_0(u - \hat{u}_h)\| + \|(I - \Pi_0)(u - \hat{u}_h)\|.$$

For the first term, by definition of L^2 projection and interpolation error, we have

$$\|\Pi_0(u - \hat{u}_h)\| = \|\Pi_0(\Pi_k u - u_h)\| \leq \|\Pi_k u - u_h\| \leq Ch^{k+3}|u|_{k+3}.$$

For the second term, we separate it into two terms using interpolation error and triangle inequality

$$\begin{aligned}\|(I - \Pi_0)(u - \hat{u}_h)\| &\leq Ch\|D(u - \hat{u}_h)\| \\ &\leq Ch\|D(u - \Pi_{k+2}u)\| + Ch\|D(\Pi_{k+2}u - \hat{u}_h)\|.\end{aligned}$$

For the first term, we can apply interpolation error:

$$Ch\|D(u - \Pi_{k+2}u)\| \leq Ch^{k+3}|u|_{k+3}.$$

For the second term, by (2.9), (2.18), and (2.12),

$$\begin{aligned}&\|D(\Pi_{k+2}u - \hat{u}_h)\|^2 \\ &= (D(\Pi_{k+2}u - u), D(\Pi_{k+2}u - \hat{u}_h)) + (Du - \Pi_{k+1}Du, D(\Pi_{k+2}u - \hat{u}_h)) \\ &+ (D_w Q_h u - D_w u_h, D(\Pi_{k+2}u - \hat{u})).\end{aligned}$$

By Cauchy-Schwarz inequality and the fact that c is positive, we have,

$$\begin{aligned}\|D(\Pi_{k+2}u - \hat{u}_h)\|^2 \leq &(\|D(\Pi_{k+2}u - u)\| + \|Du - \Pi_{k+1}Du\| + |||Q_h u - u_h|||) \\ &\cdot \|D(\Pi_{k+2}u - \hat{u}_h)\|.\end{aligned}$$

By interpolation error and (2.12),

$$\|D(\Pi_{k+2}u - \hat{u}_h)\|^2 \leq Ch^{k+2}|u|_{k+3}\|D(\Pi_{k+2}u - \hat{u}_h)\|.$$

Combining the three main inequalities, we have

$$\|u - \hat{u}_h\| \leq Ch^{k+3}|u|_{k+3} + Ch^{k+3}|u|_{k+3} + Ch^{k+3}|u|_{k+3} \leq Ch^{k+3}|u|_{k+3}.$$

□

2.4 Numerical Implementation

First we list the important notation used in this section, see Table 2.1

Table 2.1: Important notation for our numerical implementation

Notation	Explanation
A	stiffness matrix
M	mass matrix
$\Phi_i(x)$	global basis function
$\phi_i(x)$	local basis function
$m_\alpha(x)$	$m_\alpha(x) = (\frac{x-\beta}{h})^\alpha$
$\eta_1(x)$	$\eta_1(x) = \frac{1}{h}(x - x_i)$
$\eta_2(x)$	$\eta_2(x) = -\frac{1}{h}(x - x_{i+1})$
c_i	coefficients for basis functions

We can represent $D_w u$ as linear combination of monomials $m_\alpha(x)$

$$D_w u(x) = \sum_{\alpha=0}^{2} \mathsf{S}^\alpha m_\alpha(x),$$

where S is a matrix of the coefficients of $m_\alpha(x)$ to be determined later.
We can also represent u as

$$u_h(x) = \sum_{i=1}^{N} c_i \Phi_i(x).$$

For the case where there are 2 sub intervals, we will have $2 \times 2 + 3 = 7$ basis functions, see Figure 2.1.

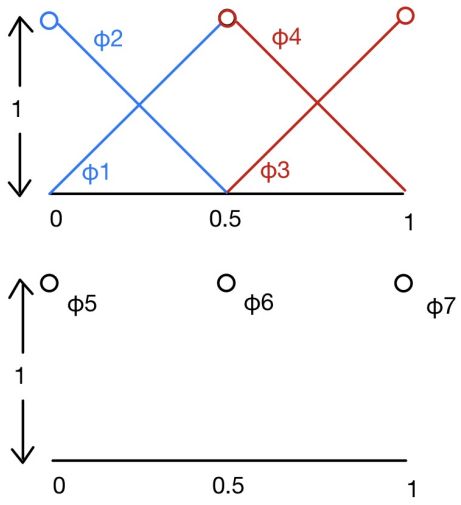

Figure 2.1: Global Indexing of the basis functions

2.4.1 Derivation the stiffness matrix

Our goal is to find coefficients c_i to represent $u_h(x)$. The strategy is to first derive the local stiffness matrix, using local basis functions $\phi_j(x)$ see Figure 2.2, then use it to construct the global stiffness matrix.

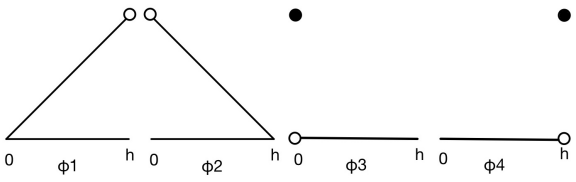

Figure 2.2: Local Indexing of the basis functions

In this section we present the method for constructing the numerical implementation. For simplicity, we consider the case where $k = 1$, and we have 2 subintervals. Let

$$D_w\phi_i(x) = \sum_\alpha \mathsf{S}_i^\alpha m_\alpha(x),\ 1 \le i \le 4,$$

define

$$\mathsf{G} := \begin{pmatrix} (m_2, m_2) & (m_1, m_2) & (m_0, m_2) \\ (m_2, m_1) & (m_1, m_1) & (m_0, m_1) \\ (m_2, m_0) & (m_1, m_0) & (m_0, m_0) \end{pmatrix}.$$

Then,

$$(D_w\phi_i(x), D_w\phi_j(x)) = \left(\sum_\alpha \mathsf{S}_i^\alpha m_\alpha(x), \sum_\alpha \mathsf{S}_i^\alpha m_\alpha(x) \right) = \mathsf{S}_i^\top G \mathsf{S}_j.$$

Using $m_\alpha(x)$'s as test functions, we can find S_i, however, it is not necessary to find S. Let $\mathbf{b_i} = \mathsf{G}\mathsf{S}_i$, then

$$(D_w\phi_i, D_w\phi_j) = \mathbf{b_i}^\top \mathsf{G}^{-1} \mathbf{b_j}. \tag{2.21}$$

We can compute $\mathbf{b_i}$ by definition:

$$(\mathbf{b_i})_\alpha = -(\phi_i, Dm_\alpha)_I + \langle \phi_i, m_\alpha \rangle_{\partial I}.$$

We find that

$$\mathsf{G} = h \begin{pmatrix} \frac{1}{5} & \frac{1}{4} & \frac{1}{3} \\ \frac{1}{4} & \frac{1}{3} & \frac{1}{2} \\ \frac{1}{3} & \frac{1}{2} & 1 \end{pmatrix},$$

$$\mathsf{B} := \begin{pmatrix} \mathbf{b_1} & \mathbf{b_2} & \mathbf{b_3} & \mathbf{b_4} \end{pmatrix} = \begin{pmatrix} -\frac{2}{3} & -\frac{1}{3} & 0 & 1 \\ -\frac{1}{2} & -\frac{1}{2} & 0 & 1 \\ 0 & 0 & -1 & 1 \end{pmatrix}.$$

Thus

$$(D_w\phi_i, D_w\phi_j) = \begin{pmatrix} 16 & -4 & 4 & -16 \\ -4 & 16 & -16 & 4 \\ 4 & -16 & 18 & -6 \\ -16 & 4 & -6 & 18 \end{pmatrix}.$$

Now we can construct the global stiffness matrix:

$$\mathsf{A} := (D_w\Phi_i, D_w\Phi_j)_{\mathcal{T}_h} = \begin{pmatrix} 16 & -4 & 0 & 0 & 4 & -16 & 0 \\ -4 & 16 & 0 & 0 & -16 & 4 & 0 \\ 0 & 0 & 16 & -4 & 0 & 4 & -16 \\ 0 & 0 & -4 & 16 & 0 & -16 & 4 \\ 4 & -16 & 0 & 0 & 18 & -6 & 0 \\ -16 & 4 & 4 & -16 & -6 & 36 & -6 \\ 0 & 0 & -16 & 4 & 0 & -6 & 18 \end{pmatrix}.$$

2.4.2 Derivation of the mass matrix

We can directly calculate the mass matrix:

$$(\Phi_1, \Phi_1)_{\mathcal{T}_h} = (\Phi_2, \Phi_2)_{\mathcal{T}_h} = (\Phi_3, \Phi_3)_{\mathcal{T}_h} = (\Phi_4, \Phi_4)_{\mathcal{T}_h} = \int_0^{\frac{1}{2}} (2x)(2x)dx = \frac{1}{6}.$$

$$(\Phi_1, \Phi_2)_{\mathcal{T}_h} = (\Phi_2, \Phi_1)_{\mathcal{T}_h} = (\Phi_3, \Phi_4)_{\mathcal{T}_h} = (\Phi_4, \Phi_3)_{\mathcal{T}_h} = \int_0^{\frac{1}{2}} (2x)(-2x+1)dx = \frac{1}{2}.$$

The terms that involve the boundary basis functions are automatically zero, because the involved basis functions have disjoint support.

$$\mathsf{M} := (\Phi_i, \Phi_j)_{\mathcal{T}_h} = \begin{pmatrix} 1/6 & 1/12 & 0 & 0 & 0 & 0 & 0 \\ 1/12 & 1/6 & 0 & 0 & 0 & 0 & 0 \\ 0 & 0 & 1/6 & 1/12 & 0 & 0 & 0 \\ 0 & 0 & 1/12 & 1/6 & 0 & 0 & 0 \\ 0 & 0 & 0 & 0 & 0 & 0 & 0 \\ 0 & 0 & 0 & 0 & 0 & 0 & 0 \\ 0 & 0 & 0 & 0 & 0 & 0 & 0 \end{pmatrix}.$$

2.4.3 Derivation of the numerical solution

Gaussian quadrature is a powerful numerical tool when it comes to approximating definite integrals. The general formula is:

$$\int_a^b g(x)dx \approx \frac{b-a}{2} \sum_{i=1}^{n} w_i g(\frac{b-a}{2}\xi_i + \frac{a+b}{2}),$$

where n is the number of quadrature points, ξ are the quadrature points, and w_i are the corresponding weights at each points. We list a few quadrature rules below in Table 2.2, the quadrature rules can be computed using the code found in [13] For a given function f, to find the numerical solution, i.e. the c_i's, we can test (2.5) by the basis functions $\Phi_i, 1 \leq i \leq 7$.

$$(\mathsf{A} + \mathsf{M})\mathbf{c}_h = \mathbf{f},$$

where $\mathbf{c}_h = [c_1,\ c_2,\ \ldots,\ c_7]^\top$ and $\mathbf{f} = [(f, \Phi_1),\ (f, \Phi_2),\ \ldots,\ (f, \Phi_7)]^\top_{[a,b]}$, i.e. the inner product between f and Φ_i on interval $[a, b]$.

We will use Gaussian quadrature to calculate $\mathbf{f}$, since we have the formula for A and M, we can solve for $\mathbf{c}_h$, and determine $u_h(x)$.

Table 2.2: Selected quadrature rules

Number of points, n	points, ξ_i	weights, w_i
1	0	2
2	$\pm\frac{1}{\sqrt{3}}$	1
3	0	$\frac{8}{9}$
	$\pm\sqrt{\frac{3}{5}}$	$\frac{5}{9}$
$\cdots$	$\cdots$	$\cdots$
7	± 0.949107912342758	0.129484966168870
	± 0.741531185599395	0.279705391489277
	± 0.405845151377397	0.381830050505119
	0	0.417959183673469

2.4.4 Derivation of the energy error

For a given $v \in V_h$, to calculate $|||v|||$ numerically, we first rewrite v in terms of Φ, i.e. $v = \sum_{i=1}^{N} v_i \Phi_i$. Thus,

$$\begin{aligned} |||v|||^2 = (D_w v, D_w v) &= (D_w \sum v_i \Phi_i, D_w \sum v_i \Phi_i) \\ &= \sum_i \sum_j v_i v_j (D_w \Phi_i, D_w \Phi_j) \\ &= [v_1\ v_2\ \cdots\ v_N](D_w \Phi_i, D_w \Phi_j)[v_1\ v_2\ \cdots\ v_N]^\top. \end{aligned}$$

i.e.

$$|||v|||^2 = [v_1\ v_2\ \cdots\ v_N]\mathsf{A}[v_1\ v_2\ \cdots\ v_N]^\top. \tag{2.22}$$

Next we want find a numerical representation of $Q_h u$; we denote the corresponding vector as $\mathbf{q}_h$. We calculate $\mathbf{q}_h$ by dividing it into two parts: the part that corresponds to $\Pi_k u$ denoted as $\mathbf{q}_{h,0}$, and the part that corresponds to u denoted as $\mathbf{q}_{h,b}$. If we restrict our attention to one sub-interval, we can calculate $\mathbf{q}_{h,0}$ on this interval:

$$\int_I (\Pi_1 u(x)) p(x)\, dx = \int_I u(x) p(x)\, dx,\ \forall p \in P_1(I).$$

Denote $\eta_1(x)$ as the monomial of degree one with slope $\frac{1}{h}$, and $\eta_2(x)$ as the monomial of degree one with slope $-\frac{1}{h}$, i.e.

$$\eta_1(x) = \frac{1}{h}(x - x_i).$$

Since $k = 1$, $\Pi_1 u(x)$ is linear, so we can use $\eta_1(x)$ and $\eta_2(x)$ as our basis functions, thus $\Pi_1 u(x) = a\eta_1(x) + b\eta_2(x)$.

Now we want to use the above relation and testing by $\eta_1(x)$ and $\eta_2(x)$ to find a and b:

$$\begin{bmatrix} (\eta_1, \eta_1)_I & (\eta_2, \eta_1)_I \\ (\eta_1, \eta_2)_I & (\eta_2, \eta_2)_I \end{bmatrix} \begin{bmatrix} a \\ b \end{bmatrix} = \begin{bmatrix} (u, \eta_1)_I \\ (u, \eta_2)_I \end{bmatrix}.$$

Since $(\eta_1, \eta_1)_I = (\eta_2, \eta_2)_I = \frac{h}{3}$, and $(\eta_2, \eta_1)_I = (\eta_1, \eta_2)_I = \frac{h}{6}$, we have

$$\mathsf{C} := \begin{bmatrix} (\eta_1, \eta_1)_I & (\eta_2, \eta_1)_I \\ (\eta_1, \eta_2)_I & (\eta_2, \eta_2)_I \end{bmatrix} = \begin{bmatrix} \frac{h}{3} & \frac{h}{6} \\ \frac{h}{6} & \frac{h}{3} \end{bmatrix}.$$

We then use 7- points Gaussian Quadrature combined with similar triangles to calculate the right-hand-side: $\texttt{temp 1} := \int_I u(x)\eta_1(x)\,dx$

$$\int_0^1 u(x)\eta_1(x)\,dx \approx \frac{1}{2}\sum_{i=1}^{7} w_i u(\frac{1}{2}\xi_i + \frac{1}{2})\eta_1(\frac{1}{2}\xi_i + \frac{1}{2}),$$

where w_i's are the the Gaussian quadrature weights defined before, and the ξ_i's are the corresponding quadrature points. We can use similar triangle to calculate η_1 and η_2 at the desired points, and we can use the exact solution to calculate $u(\frac{1}{2}\xi_i + \frac{1}{2})$. Similarly, we can calculate $\texttt{temp 2} := \int_I u(x)\eta_2(x)\,dx$. Thus, on one interval we have:

$$\mathsf{C}\begin{bmatrix} a \\ b \end{bmatrix} = \begin{bmatrix} \texttt{temp 1} \\ \texttt{temp 2} \end{bmatrix}.$$

Now if we look at the whole interval $[0, 1]$, where we have 2 subintervals, we'll have

$$\begin{bmatrix} a_1 & a_2 \\ b_1 & b_2 \end{bmatrix} = \mathsf{C}^{-1}\begin{bmatrix} \texttt{temp 1}' \\ \texttt{temp 2}' \end{bmatrix} = \mathsf{T}.$$

We know that a_i and b_i are the actual function values at the end of each subinterval for $\Pi_1 u(x)$; thus they can serve as the components for $\mathbf{q}_{h,0}$. By using the exact solution for u at the interior points, we can find $\mathbf{q}_{h,b}$. We can arrange the two components in a way that matches the ordering of the $\mathbf{c}_h$.

Since $u_h = \sum_i^N c_i\Phi_i$, to calculate $|||Q_h u - u_h|||$ numerically, we simply replace $[v_1\ v_2\ \cdots\ v_N]$ in (2.22) by $\mathbf{q}_h - \mathbf{c}_h$. Thus

$$|||Q_h u - u_h|||^2 = (\mathbf{q}_h - \mathbf{c}_h)\mathsf{A}(\mathbf{q}_h - \mathbf{c}_h)^\top.$$

2.4.5 Derivation of the L^2 error

We adopt a similar strategy to the previous section. To calculate the L^2 error numerically, we need to first find the corresponding vectors of $\Pi_k u$ and u_0. We already defined $\mathbf{q}_{h,0}$; we now define $\mathbf{c}_0$ as the part of vector $\mathbf{c}_h$ that corresponds to the interior. Thus, we want to calculate $\|\mathbf{q}_{h,0} - \mathbf{c}_0\|^2$. Given that $v = \sum v_i\Phi_i$,

$$\begin{aligned} \|v\|^2 = (v, v) &= (\sum v_i\Phi_i, \sum v_i\Phi_i) \\ &= \sum_i \sum_j v_i v_j(\Phi_i, \Phi_j) \\ &= [v_1\, v_2\, \cdots\, v_N]\mathsf{M}[v_1\, v_2\, \cdots\, v_N]^\top. \end{aligned}$$

Thus,

$$\|\mathbf{q}_{h,0} - \mathbf{c}_0\|^2 = (\mathbf{q}_{h,0} - \mathbf{c}_0)\mathsf{M}(\mathbf{q}_{h,0} - \mathbf{c}_0)^\top.$$

Since we know the mass matrix has zero entries on the boundary of each interval, we can simply use $(\mathbf{q}_h - \mathbf{c}_h)\mathsf{M}(\mathbf{q}_h - \mathbf{c}_h)^\top$ to calculate the L^2 error numerically.

2.4.6 Derivation of the lifted solution and its L^2 error

For the numerical implementation for (2.18)-(2.19), since $k = 1$, we are looking for a lifted solution in P_3. On each subinterval, there are four relevant basis functions. Let

$$\hat{u}_h(x) = \sum_{\alpha=0}^{3} \hat{u}^\alpha m_\alpha(x) \quad \text{and} \quad D_w u_h(x) = \sum_{k=1}^{4} D_w(c_k \Phi_k(x)).$$

From (2.18)-(2.19), we test $D\hat{u}_h$ by monomials up from degree one to degree three, and testing $\hat{u}_h$ by constant one, for the left hand side we get:

$$\begin{bmatrix} (Dm_3, Dm_3) & (Dm_2, Dm_3) & (Dm_1, Dm_3) & (Dm_0, Dm_3) \\ (Dm_3, Dm_2) & (Dm_2, Dm_2) & (Dm_1, Dm_2) & (Dm_0, Dm_2) \\ (Dm_3, Dm_1) & (Dm_2, Dm_1) & (Dm_1, Dm_1) & (Dm_0, Dm_1) \\ (m_3, 1) & (m_2, 1) & (m_1, 1) & (m_0, 1) \end{bmatrix} \begin{bmatrix} \hat{u}_3 \\ \hat{u}_2 \\ \hat{u}_1 \\ \hat{u}_0 \end{bmatrix}$$

$$= \frac{1}{h} \begin{bmatrix} \frac{9}{5} & \frac{6}{4} & 1 & 0 \\ \frac{6}{4} & \frac{4}{3} & 1 & 0 \\ 1 & 1 & 1 & 0 \\ \frac{h^2}{4} & \frac{h^2}{3} & \frac{h^2}{2} & h^2 \end{bmatrix} \begin{bmatrix} \hat{u}_3 \\ \hat{u}_2 \\ \hat{u}_1 \\ \hat{u}_0 \end{bmatrix}.$$

For the right hand side, on each subinterval we have

$$\begin{aligned} D_w u_h = D_w \left(\sum_{k=1}^{4} (c_k \Phi_k) \right) &= \sum_{k=1}^{4} c_k (D_w \Phi_k) \\ &= \sum_{k=1}^{4} c_k \sum_{\alpha=0}^{2} (\mathsf{S}_k^\alpha m_\alpha) \\ &= \left(\mathsf{S}_4^2 c_4 + \mathsf{S}_3^2 c_3 + \mathsf{S}_3^2 c_2 + \mathsf{S}_1^2 c_1 \right) m_2 \\ &\quad + \left(\mathsf{S}_4^1 c_4 + \mathsf{S}_3^1 c_3 + \mathsf{S}_2^1 c_2 + \mathsf{S}_1^1 c_1 \right) m_1 \\ &\quad + \left(\mathsf{S}_4^0 c_4 + \mathsf{S}_3^0 c_3 + \mathsf{S}_2^0 c_2 + \mathsf{S}_1^0 c_1 \right) m_0. \end{aligned}$$

We can denote this as $D_w u_h = r_2 m_2 + r_1 m_1 + r_0 m_0$. Testing $D_w u_h$ by the same monomials as we did for $D\hat{u}_h$, we have

$$\begin{bmatrix} (D_w u_h, Dm_3) \\ (D_w u_h, Dm_2) \\ (D_w u_h, Dm_1) \end{bmatrix} = \begin{bmatrix} (m_2, Dm_3) & (m_1, Dm_3) & (m_0, Dm_3) \\ (m_2, Dm_2) & (m_1, Dm_2) & (m_0, Dm_2) \\ (m_2, Dm_1) & (m_1, Dm_1) & (m_0, Dm_1) \end{bmatrix} \begin{bmatrix} r_2 \\ r_1 \\ r_0 \end{bmatrix}$$

$$= \frac{1}{h} \begin{bmatrix} \frac{3}{5} & \frac{3}{4} & 1 \\ \frac{2}{4} & \frac{2}{3} & 1 \\ \frac{1}{3} & \frac{1}{2} & 1 \end{bmatrix} \begin{bmatrix} r_2 \\ r_1 \\ r_0 \end{bmatrix}.$$

Furthermore,

$$\begin{bmatrix} r_2 \\ r_1 \\ r_0 \end{bmatrix} = \begin{bmatrix} \mathsf{S}_4^2 & \mathsf{S}_3^2 & \mathsf{S}_2^2 & \mathsf{S}_1^2 \\ \mathsf{S}_4^1 & \mathsf{S}_3^1 & \mathsf{S}_2^1 & \mathsf{S}_1^1 \\ \mathsf{S}_4^0 & \mathsf{S}_3^0 & \mathsf{S}_2^1 & \mathsf{S}_1^0 \end{bmatrix} \begin{bmatrix} c_4 \\ c_3 \\ c_2 \\ c_1 \end{bmatrix}.$$

We can find S by matrix B and G in (2.21). Testing u_h by constant one, we have $(u_h, 1) = \int_I c_1\Phi_1 dx + \int_I c_2\Phi_2 dx = \frac{c_1+c_2}{2}h$. By setting both side equal to each other, we can solve for the coefficients $\hat{u}^\alpha$. Finally, given the exact solution, we can use Gaussian quadrature to calculate $\|u - \hat{u}_h\|$.

2.5 Numerical Experiments

In this section, we examine the stabilizer free WG method by testing its accuracy and convergence order for solving diffusion-reaction equation. For convergence tests, we consider linear basis functions, i.e. $k = 1$. The mesh generation and all computations are conducted in the MATLAB environment defined by following above section. For simplicity, we only use uniform mesh size, even though the WG method is known to be very good at handling different finite element partitions [9, 8]. We are expecting order 3 superconvergence for the energy norm error, and order 4 superconvergence for the L^2 norm error. As for the L^2 norm of the lifted solution, we expect order 4 superconvergence . We present several examples here.

2.5.1 Example 1: Quadratic polynomial solution

In this test, let $\Omega = (0, 1)$, and we solve the following equation:

$$-u'' + u = x^2 - x - 2,$$
$$u(0) = u(1) = 0.$$

The exact solution to this problem is

$$u(x) = x^2 - x. \tag{2.23}$$

Applying the stabilizer free WG finite element method, we achieve the results in Table 2.3. As we can see, our method achieves machine zero error for the energy norm, L^2 norm, and the L^2 norm for the lifted solution. Thus, for quadratic exact solutions, the proposed method can compute the solution exactly.

Table 2.3: Error profiles and convergence rates for solution (2.24)

Grid	$\|\Pi_1 u - u_0\|$	rate	$\|\|\|Q_h u - u_h\|\|\|$	rate
2	$1.3741e-15$	N/A	$4.7320e-15$	N/A
3	$1.8958e-15$	N/A	$7.1890e-15$	N/A
4	$6.4547e-15$	N/A	$2.1877e-14$	N/A
Grid	$\|u - u_h\|$	rate	$\|u - \hat{u}_h\|$	rate
2	$4.6585e-03$	2	$1.3682e-15$	N/A
3	$1.1646e-03$	2	$1.8728e-15$	N/A
4	$2.9115e-04$	2	$6.4172e-15$	N/A
5	$7.2789e-05$	2	$2.5560e-14$	N/A
6	$1.8197e-05$	2	$1.1508e-13$	N/A

2.5.2 Example 2: Cubic polynomial solution

In this test, let $\Omega = (0, 1)$, and we solve the following equation:

$$-u'' + u = x^3 - 7x,$$
$$u(0) = u(1) = 0.$$

The exact solution to this problem is

$$u(x) = x^3 - x. \tag{2.24}$$

Similarly to previous example, by applying stabilizer free WG finite element method, we achieve the results in Table 2.4. As we can see, our method achieves machine zero error for the energy norm, L^2 norm, and the L^2 norm for the lifted solution. Thus, for cubic exact solutions, the proposed method can compute the solution exactly.

Table 2.4: Error profiles and convergence rates for solution (2.24)

Grid	$\|\Pi_1 u - u_0\|$	rate	$\|\|\|Q_h u - u_h\|\|\|$	rate
2	$2.0155e-15$	N/A	$7.0125e-15$	N/A
3	$2.8324e-15$	N/A	$1.0640e-14$	N/A
4	$1.0134e-14$	N/A	$3.4275e-14$	N/A
Grid	$\|u - u_h\|$	rate	$\|u - \hat{u}_h\|$	rate
2	$8.0109e-03$	2	$1.9202e-15$	N/A
3	$2.0136e-03$	2	$2.7845e-15$	N/A
4	$5.0407e-04$	2	$1.0075e-14$	N/A
5	$1.2606e-04$	2	$3.7842e-14$	N/A
6	$3.1518e-05$	2	$1.7452e-13$	N/A

2.5.3 Example 3: Quartic polynomial solution

In this test, let $\Omega = (0, 1)$, and we solve the following equation:

$$-u'' + u = x^4 - 14x^2 + 2,$$
$$u(0) = u(1) = 0.$$

The exact solution to this problem is

$$u(x) = x^4 - x^2. \tag{2.25}$$

By applying stabilizer free WG finite element method, we observe the desired convergence order in Table 2.5. It can be seen that the weak solution has convergence of order three for energy norm and order four for L^2 norm. We can also observe that the error of the lifted solution has order four convergence, comparing to the order two convergence of the non-lifted solution. A more straightforward representation of the convergence order can be found in Figure 2.3; this graph is generated by using code developed in [2]. The ratio between the change in the exponent for the y axis and the change in the exponent for the x axis represent the order of convergence. As we can see, when the mesh size is too small, the convergence order may decrease due to machine precision.

Table 2.5: Error profiles and convergence rates for solution (2.25)

Grid	$\|\Pi_1 u - u_0\|$	rate	$\|\|\|Q_h u - u_h\|\|\|$	rate
2	$1.2042e-04$	4	$1.7999e-03$	3
3	$7.5264e-06$	4	$2.2539e-04$	3
4	$4.7040e-07$	4	$2.8187e-05$	3
5	$2.9400e-08$	4	$3.5237e-06$	3
6	$1.8374e-09$	4	$4.4048e-07$	3
Grid	$\|u - u_h\|$	rate	$\|u - \hat{u}_h\|$	rate
2	$9.2462e-03$	2	$1.4738e-04$	4
3	$2.3680e-03$	2	$9.2187e-06$	4
4	$5.9552e-04$	2	$5.7629e-07$	4
5	$1.4910e-04$	2	$3.6020e-08$	4
6	$3.7289e-05$	2	$2.2512e-09$	4

2.5.4 Example 4: Trigonometric solution

In this test, let $\Omega = (0, 1)$, and we solve the following equation:

$$-u'' + u = \pi^2(\sin \pi x) + \sin(\pi x),$$
$$u(0) = u(1) = 0.$$

The exact solution to this problem is

$$u(x) = \sin(\pi x). \tag{2.26}$$

By applying stabilizer free WG finite element method, we observe the desired convergence order in Table 2.6. It can be seen that the weak solution has convergence order of order three for energy norm and order four for L^2 norm. In Figure 2.4 we plot the figure of the exact solution in red and the numerical solution in blue and *, to compare and observe how the performance improves as we refine the mesh size. We can also observe that the error of the lifted solution has order four convergence, comparing to the order two convergence of the non-lifted solution.

Remark 2.5.1. *As we can see, the L^2 norm of the difference between the exact solution and numerical solution has order one convergence. That is due to the interpolation error. By triangle inequality:*

$$\|u - u_h\| \leq \|u - \Pi_1 u\| + \|\Pi_1 u - u_h\|,$$

where the first term has second order convergence and second term is proven to be fourth order convergent. Whereas the the L^2 norm of the difference between the exact solution and the numerical solution has order four superconvergence.

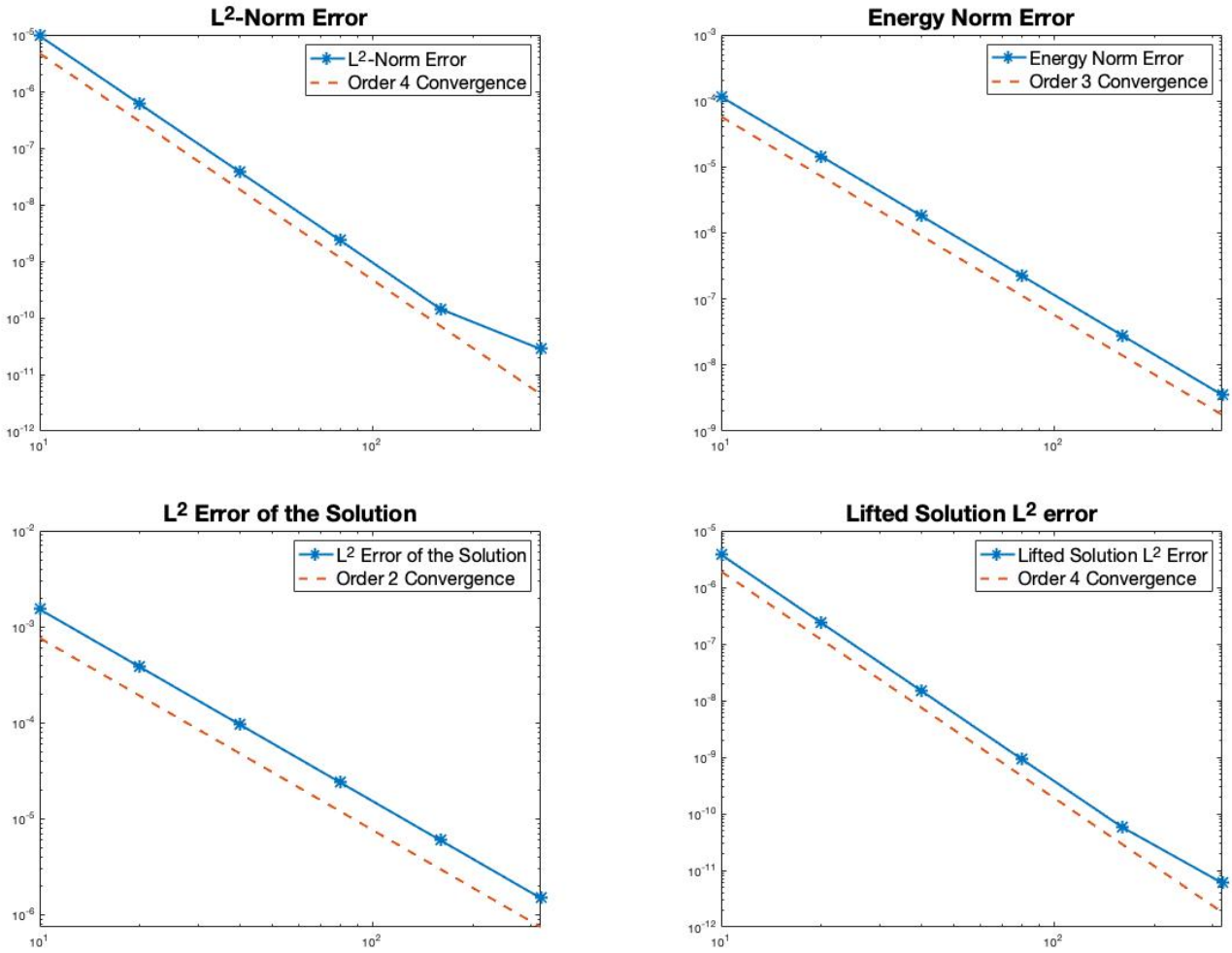

Figure 2.3: Convergence Rate for solution (2.25)

2.5.5 Example 5: Trigonometric solution with non-homogeneous boundary condition

In this test, let $\Omega = [0, 1]$, and we solve the following equation:

$$\begin{aligned} -u'' + u &= \pi^2(\cos(\pi x)) + \cos(\pi x), \\ u(0) &= 1, \\ u(1) &= -1. \end{aligned}$$

The exact solution to this problem is

$$u(x) = \cos(\pi x). \tag{2.27}$$

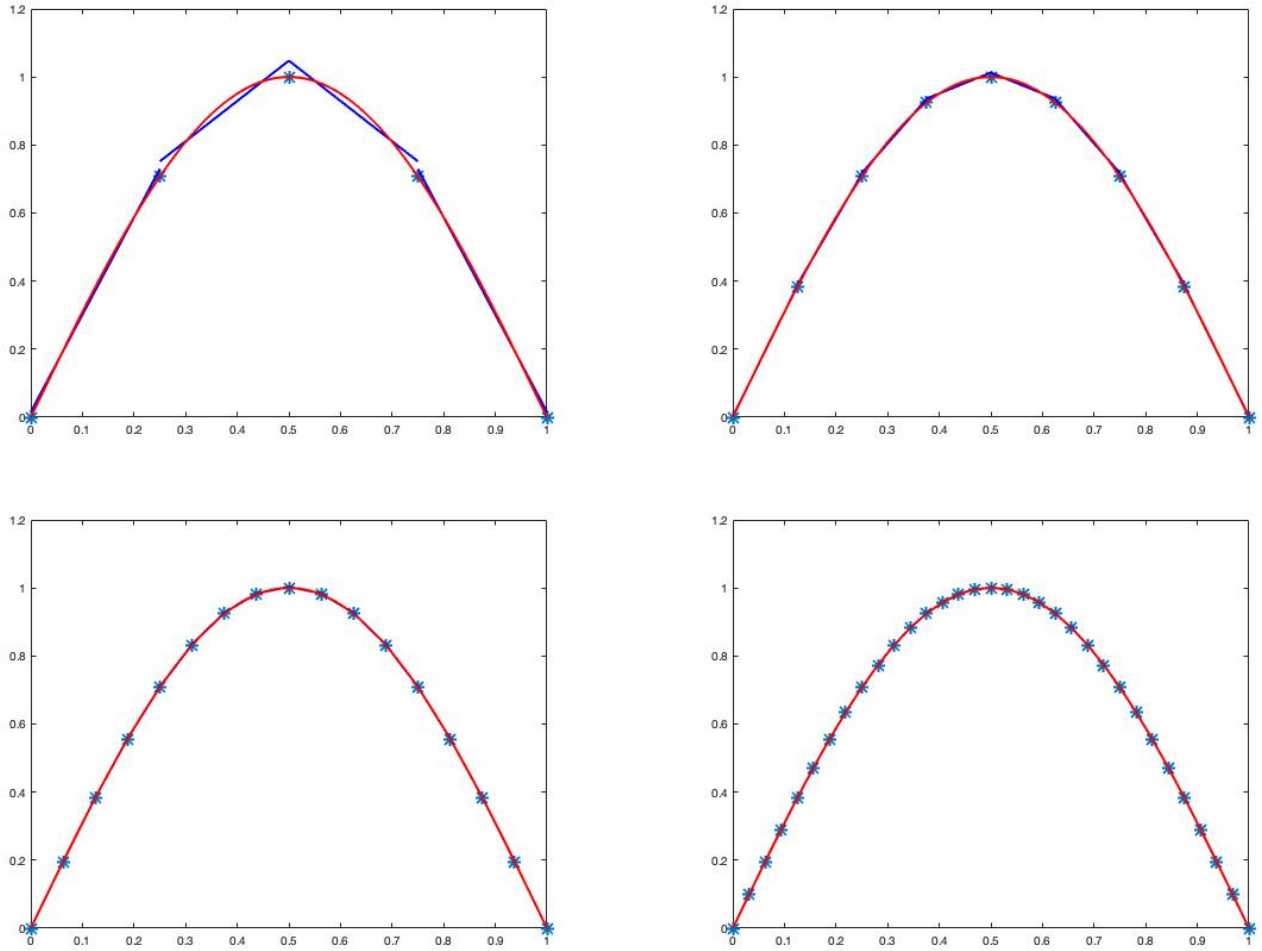

Figure 2.4: Plot of Exact Solution and Numerical Solution of solution (2.26)

Our method also works for non-homogeneous boundary condition. In this example, we test the method by using non-homogeneous Dirichlet boundary condition. We observe the desired convergence order in Table 2.7. It can be seen that the weak solution has convergence order of order three for energy norm and order four for L^2 norm.

Table 2.6: Error profiles and convergence rates for solution (2.26)

Grid	$\|\Pi_1 u - u_0\|$	rate	$\|\|\|Q_h u - u_h\|\|\|$	rate
2	$1.2042e-04$	4	$5.1139e-03$	3
3	$7.5264e-06$	4	$6.4524e-04$	3
4	$4.7040e-07$	4	$8.0843e-05$	3
5	$2.9400e-08$	4	$1.0111e-05$	3
6	$1.8374e-09$	4	$1.2641e-06$	3
Grid	$\|u - u_h\|$	rate	$\|u - \hat{u}_h\|$	rate
2	$1.6116e-02$	2	$4.1472e-04$	4
3	$4.0550e-03$	2	$2.6089e-05$	4
4	$1.0154e-03$	2	$1.6331e-06$	4
5	$2.5396e-04$	2	$1.0211e-07$	4
6	$6.3496e-05$	2	$6.3830e-09$	4

Table 2.7: Error profiles and convergence rates for solution (2.27)

Grid	$\|\Pi_1 u - u_0\|$	rate	$\|\|\|Q_h u - u_h\|\|\|$	rate
2	$3.6294e-04$	4	$5.1130e-03$	3
3	$2.2861e-05$	4	$6.4521e-04$	3
4	$1.4315e-06$	4	$8.0843e-05$	3
5	$8.9514e-08$	4	$1.0111e-05$	3
6	$5.5954e-09$	4	$1.2641e-06$	3
Grid	$\|u - u_h\|$	rate	$\|u - \hat{u}_h\|$	rate
2	$1.6117e-02$	2	$4.3593e-04$	4
3	$4.0550e-03$	2	$2.7476e-05$	4
4	$1.0154e-03$	2	$1.7208e-06$	4
5	$2.5396e-04$	2	$1.0760e-07$	4
6	$6.3496e-05$	2	$6.7262e-09$	4

Chapter 3

A Superconvergent weak Galerkin finite element method for two dimensional reaction-diffusion equations

3.1 Preliminaries and Notations

In this section, we define the mesh, the definition of the stabilizer free weak Galerkin finite element space, and the weak gradient. For the 2-D problem, we consider the square domain of $\Omega = [a, b] \times [c, d]$.

Let $\Omega = [a, b] \times [c, d] = \cup_{i=1}^{N} T_i$, with T_i being triangles, and $\mathcal{T}_h = \{T_i | i = 1, \cdots, N\}$, where h is the largest side length of all triangles. We also define h_T as the diameter of the triangle T.

For a given integer $k \geq 1$, let V_h be the weak Galerkin finite element space associated with $\mathcal{T}_h$ defined as follows

$$V_h = \{v = \{v_0, v_b\} : v_0|_T \in P_k(T), v_b|_e \in P_{k+1}(e), \forall e \subseteq \partial T, \forall T \in \mathcal{T}_h, v_b|_{\partial\Omega} = 0\}. \tag{3.1}$$

For simplicity, in this section, we only consider the case $k = 1$, i.e.

$$V_h = \{v = \{v_0, v_b\} : v_0|_T \in P_1(T), v_b|_e \in P_2(e), \forall e \subseteq \partial T, \forall T \in \mathcal{T}_h, v_b|_{\partial\Omega} = 0\}. \tag{3.2}$$

Next, we define the weak derivative for the case where $k = 1$:

Definition 3.1.1. *For $v \in V_h$, the weak derivative $\nabla_w v$ is a piecewise polynomial such that on each T, $\nabla_w v \in (P_2(T))^2$ satisfies:*

$$\int_T \nabla_w v \cdot \mathbf{q} d\mathbf{x} = \sum_{e \subseteq \partial T} \int_e v_b (\mathbf{q} \cdot \mathbf{n}) ds - \int_T v_0 (\nabla \cdot \mathbf{q}) d\mathbf{x}, \quad \forall \mathbf{q} \in (P_2(T))^2. \tag{3.3}$$

3.2 Numerical Scheme and Wellposedness

We consider the same problem (1.1)-(1.2) but in 2-D.

Algorithm 3.2.1. *A SFWG method for problem (1.1)-(1.2) seeks $u_h \in V_h$ satisfying the following equation:*

$$(\nabla_w u_h, \nabla_w v) + c(u_0, v_0) = (f, v_0), \quad \forall v \in V_h. \tag{3.4}$$

For any $v \in V_h$, we define 2 semi-norms using notation in 2-D:

$$|||v|||^2 = (\nabla_w v, \nabla_w v) + c\|v_0\|^2, \tag{3.5}$$

$$\|v\|_{1,h}^2 = \sum_{T\in\mathcal{T}_h} (\|\nabla v_0\|_T^2 + h_T^{-1}\|v_0 - v_b\|_e^2) + c\|v_0\|^2. \tag{3.6}$$

First, we want to establish that $|||\cdot|||$ is a norm, i.e. if $|||v||| = 0$, then $v = 0$.

Remark 3.2.1. *If $|||v||| = 0$, then $\nabla_w v = 0$ Since c is positive constant, by. (3.3), we have*

$$\sum_{e\subseteq\partial T}\int_e v_b(\mathbf{q}\cdot\mathbf{n})ds - \int_T v_0(\nabla\cdot\mathbf{q})d\mathbf{x} = 0, \quad \forall \mathbf{q} \in (P_2(T))^2.$$

We can find $\mathbf{q}$ s.t. $\mathbf{q}\cdot\mathbf{n}|_e = 0$ and $\nabla\cdot\mathbf{q} = v_0$. Thus, $\int_T (v_0)^2 d\mathbf{x} = 0$, i.e. $v_0 = 0$. Similarly, we can find $\mathbf{q}$ s.t. $\nabla\cdot\mathbf{q} = 0$, with $\mathbf{q}\cdot\mathbf{n}|_e = v_b$. $\sum_{e\subseteq\partial T}\int_e v_b^2 ds = 0$, thus $v_b = 0$. Thus $v_0 = v_b = 0$, i.e. $v = 0$ if $|||v||| = 0$.

Theorem 3.2.1. *There exists a positive constant C, independent of h, such that for any $v \in V_h$, we have*

$$\|v\|_{1,h} \le C|||v|||. \tag{3.7}$$

Proof. By similar argument as in the one dimensional case, we can pick $\mathbf{q}$ such that $\mathbf{q}\cdot\mathbf{n} = h_T^{-1}(v_b - v_0)$ and $(\mathbf{q}, \nabla v_0) = (\nabla v_0, \nabla v_0) + c(v_0, v_0)$. By definition of the weak derivative (3.3), integration by parts, and the properties for $\mathbf{q}$, we have

$$\begin{aligned}
(\nabla_w v, \mathbf{q}) &= \sum_{T\in\mathcal{T}_h}\left[\sum_{e\subseteq\partial T}\int_e v_b(\mathbf{q}\cdot\mathbf{n})ds - \int_T v_0(\nabla\cdot\mathbf{q})d\mathbf{x}\right] \\
&= \sum_{T\in\mathcal{T}_h}\left[\sum_{e\subseteq\partial T}\int_e v_b(\mathbf{q}\cdot\mathbf{n}) - \left[\sum_{e\subseteq\partial T}(v_0, \mathbf{q}\cdot\mathbf{n}) - (\mathbf{q}, \nabla v_0)_T\right] ds\right] \\
&= \sum_{T\in\mathcal{T}_h}\left[\sum_{e\subseteq\partial T}(v_b - v_0, \mathbf{q}\cdot\mathbf{n})_e + (\nabla v_0, \nabla v_0)_T + c(v_0, v_0)\right] \\
&= \sum_{T\in\mathcal{T}_h}\left(\|\nabla v_0\|_T^2 + c\|v_0\|_T^2 + h_T^{-1}\|v_0 - v_b\|_e^2\right) \\
&= \|v\|_{1,h}^2.
\end{aligned}$$

By the finite dimensional norm equivalence,

$$\|\mathbf{q}\| \le C\|v\|_{1,h}.$$

Given that c is a positive constant,

$$\|v\|_{1,h}^2 = (\nabla_w v, \mathbf{q}) \le \|\nabla_w v\|\|\mathbf{q}\| \le C|||v|||\|v\|_{1,h}.$$

□

This implies that $\|\cdot\|_{1,h}$ is also a norm. This justifies the well-poseness of the scheme.

3.3 Error Analysis

3.3.1 Error Equations

In this section, we establish some useful lemmas for error estimates. First, let $\Pi_2 u$ be the L^2 projection from $(L^2(T))^2$ to $(P_2(T))^2$. Define $Q_h u$ as follows: $Q_h u = \begin{cases} Q_0 u, & \text{on } T \\ Q_b u, & \text{on } e \end{cases}$, where $Q_0 u \in P_1(T)$ and $Q_b u \in P_2(e)$, $(Q_0 u, q)_T = (u_0, q)_T$ and $(Q_b u, p)_e = (u_b, p)_e$ for all $q \in P_1(T)$ and all $p \in P_2(e)$.

Lemma 3.3.1. *Let* $\mathbf{q}$ *be any vector in* $(P_2(T))^2$*. We have*

$$(\nabla_w (Q_h u), \mathbf{q}) = (\Pi_2 \nabla u, \mathbf{q})_T.$$

Proof. By the definition of the weak derivative (3.3), we have,

$$\begin{aligned}(\nabla_w Q_h u, \mathbf{q}) &= \sum_{e \subseteq \partial T} \int_e Q_b u (\mathbf{q} \cdot \mathbf{n}) ds - \int_T Q_0 u (\nabla \cdot \mathbf{q}) d\mathbf{x} \\ &= \sum_{e \subseteq \partial T} (Q_b u, \mathbf{q} \cdot \mathbf{n})_e - (Q_0 u, \nabla \cdot \mathbf{q})_T.\end{aligned}$$

We can then apply the definition of $Q_h u$ to both of the terms, we have

$$\sum_{e \subseteq \partial T} (Q_b u, \mathbf{q} \cdot \mathbf{n})_e - (Q_0 u, \nabla \cdot \mathbf{q})_T = -(u_0, \nabla \cdot \mathbf{q})_T + \sum_{e \subseteq \partial T} (u_b, \mathbf{q} \cdot \mathbf{n})_e.$$

Applying integration by parts, and using the definition of $\Pi_2 u$, we have

$$\begin{aligned}&- (u_0, \nabla \cdot \mathbf{q})_T + \sum_{e \subseteq \partial T} (u_b, \mathbf{q} \cdot \mathbf{n})_e \\ &= (\nabla u, \mathbf{q})_T \\ &= (\Pi_2 \nabla u, \mathbf{q})_T.\end{aligned}$$

Thus

$$(\nabla_w (Q_h u), \mathbf{q}) = (\Pi_2 \nabla u, \mathbf{q})_T.$$

□

Let $e_h = Q_h u - u_h \in V_h$. Next, we derive an error equation that e_h satisfies.

Lemma 3.3.2. *For any* $v \in V_h$*, the following error equation holds true*

$$(\nabla_w e_h, \nabla_w v) + c(u - u_0, v_0) = l(u, v) \tag{3.8}$$

where

$$l(u, v) = \sum_{T \in \mathcal{T}_h} (v_0 - v_b, \nabla u \cdot \mathbf{n} - \Pi_2 \nabla u \cdot \mathbf{n})_{\partial T}.$$

Proof. By integration by parts,

$$\sum_{T \in \mathcal{T}_h} -(\Delta u, v_0)_T = \sum_{T \in \mathcal{T}_h} \left(- \sum_{e \subseteq \partial T} (v_0, \nabla u \cdot \mathbf{n})_e + (\nabla u, \nabla v_0)_T \right).$$

Using the fact that

$$\sum_{T\in\mathcal{T}_h}(\sum_{e\subseteq\partial T}(v_b,\nabla u\cdot\mathbf{n})_e)=0,$$

we have

$$\sum_{T\in\mathcal{T}_h}-(\Delta u,v_0)=\sum_{T\in\mathcal{T}_h}\left[(\nabla u,\nabla v_0)_T-\sum_{e\subseteq\partial T}((v_0-v_b),\nabla u\cdot\mathbf{n})_e\right].$$

By the definition of Π_2 and integration by parts, we also have

$$\begin{aligned}(\nabla u,\nabla v_0)_T&=(\Pi_2\nabla u,\nabla v_0)_T\\&=\sum_{e\subseteq\partial T}(v_0-\Pi_2\nabla u\cdot\mathbf{n})_e-(v_0,\nabla\Pi_2\nabla u)_T.\end{aligned}$$

By the definition of weak derivative (3.3) ,

$$(\nabla_w v,\Pi_2\nabla u)_T=\sum_{e\subseteq\partial T}(v_b,\Pi_2\nabla u\cdot\mathbf{n})_e-(v_0,\nabla\Pi_2\nabla u)_T.$$

Thus,

$$(\nabla u,\nabla v_0)_T=(\nabla_w v,\Pi_2\nabla u)_T+\sum_{e\subseteq\partial T}(v_0-v_b,\Pi_2\nabla u\cdot\mathbf{n})_e.$$

By Lemma (3.3.1), with $\nabla_w v\in[P_2(T)]^2$,

$$(\nabla u,\nabla v_0)_T=(\nabla_w v,\nabla_w Q_h u)_T+\sum_{e\subseteq\partial T}(v_0-v_b,\Pi_2\nabla u\cdot\mathbf{n})_e.$$

Thus,

$$\begin{aligned}\sum_{T\in\mathcal{T}_h}(-(\Delta u,v_0))&=\sum_{T\in\mathcal{T}_h}\left[(\nabla_w v,\nabla_w Q_h u)_T-\sum_{e\subseteq\partial T}(v_0-v_b,\nabla u\cdot\mathbf{n}-\Pi_2\nabla u\cdot\mathbf{n})_e\right]\\&=\sum_{T\in\mathcal{T}_h}(\nabla_w v,\nabla_w Q_h u)_T-\sum_{T\in\mathcal{T}_h}(v_0-v_b,\nabla u\cdot\mathbf{n}-\Pi_2\nabla u\cdot\mathbf{n})_{\partial T}\\&=:\sum_{T\in\mathcal{T}_h}(\nabla_w v,\nabla_w Q_h u)_T-l(u,v).\end{aligned}$$

We have

$$(-\Delta u+cu,v_0)=(\nabla_w v,\nabla_w Q_h u)-l(u,v)+c(u,v_0)=(f,v_0);$$

thus

$$(\nabla_w v,\nabla_w Q_h u)=(f,v_0)-c(u,v_0)+l(u,v).$$

Subtracting (3.4), we have

$$(\nabla_w e_h,\nabla_w v)=l(u,v)-c(u-u_0,v_0).$$

This proves the theorem. □

3.3.2 Error Estimates in Energy Norm

For simplicity, we assume $k=1$ in this section. We find the upper bound for the energy norm error by finding an upper bound for $l(u,v)$.

Lemma 3.3.3. *Let u be the solution to the diffusion-reaction equation, then $u \in H^4(\Omega)$ and $v \in V_h$. There exists a constant C such that*

$$|l(u,v)| \leq Ch^3|u|_4|||v|||. \tag{3.9}$$

Proof. Since

$$l(u,v) = \sum_{T\in\mathcal{T}_h} (v_0 - v_b, \nabla u\cdot\mathbf{n} - \Pi_2\nabla u\cdot\mathbf{n})_{\partial T},$$
$$|l(u,v)| \leq \sum_{T\in\mathcal{T}_h} \Big|(v_0 - v_b, \nabla u\cdot\mathbf{n} - \Pi_2\nabla u\cdot\mathbf{n})_{\partial T}\Big|.$$

By Cauchy-Schwarz inequality, we have

$$\begin{aligned}|l(u,v)| &\leq \sum_{T\in\mathcal{T}_h} \|v_0 - v_b\|_{\partial T}\|\nabla u\cdot\mathbf{n} - \Pi_2\nabla u\cdot\mathbf{n}\|_{\partial T}\\ &\leq \left(\sum_{T\in\mathcal{T}_h} h_T^{-1}\|v_0 - v_b\|^2_{\partial T}\right)^{\frac{1}{2}}\left(\sum_{T\in\mathcal{T}_h} h_T\|\nabla u\cdot\mathbf{n} - \Pi_2\nabla u\cdot\mathbf{n}\|^2_{\partial T}\right)^{\frac{1}{2}}.\end{aligned}$$

It is easy to see the first term is less than or equal to the norm $\|v\|_{1,h}$; by (3.7), the first term is smaller than the energy norm of v. We can apply trace inequality

$$\|v\|^2_{\partial T} \leq C(h_T^{-1}\|v\|^2_T + h_T\|\nabla v\|^2_T) \tag{3.10}$$

to the second term, and use interpolation error on the result. We have

$$\begin{aligned}&\left(\sum_{T\in\mathcal{T}_h} h_T\|\nabla u\cdot\mathbf{n} - \Pi_2\nabla u\cdot\mathbf{n}\|^2_{\partial T}\right)^{\frac{1}{2}}\\ &\leq [\sum_{T\in\mathcal{T}_h} h_T(h_T^{-1}\|\nabla u\cdot n - \vec{\Pi_2\nabla u}\cdot\mathbf{n}\|^2_T + h_T\|\nabla(\nabla u\cdot\mathbf{n} - \Pi_2\nabla u\cdot\mathbf{n})\|^2_T)]^{\frac{1}{2}}\\ &\leq (\sum_{T\in\mathcal{T}_h}(Ch_Th_T^6|u|_{4,T} + Ch_T^2h_T^4|u|_{4,T}))^{\frac{1}{2}}\\ &\leq Ch^3|u|_{4,\Omega}.\end{aligned}$$

Thus,

$$|l(u,v)| \leq Ch^3|u|_4|||v|||.$$

□

Theorem 3.3.1. *Let $u_h \in V_h$ be the SFWG finite element solution of (3.4). There exists a constant C such that*

$$|||Q_hu - u_h||| \leq Ch^3|u|_4. \tag{3.11}$$

Proof. By letting $v = e_h$ in (3.8), we have

$$\begin{aligned}l(u,e_h) &= (\nabla_we_h, \nabla_we_h) + c(u - u_0, Q_0u - u_0)\\ &= (\nabla_we_h, \nabla_we_h) + c(Q_0u - u_0, Q_0u - u_0).\end{aligned}$$

Thus, since $\|\nabla_we_h\|^2$ and $c\|Q_0u - u_0\|^2$ are both positive, and by (3.9), we have

$$|||e_h|||^2 = |l(u,e_h)| \leq Ch^3|u|_4|||e_h|||,$$

which implies (3.11). □

3.3.3 Error Estimates in the L^2 Norm

The considered dual problem seeks $\Phi \in H_0^1(\Omega)$, and $\Phi = 0$ on the boundary of Ω satisfying

$$-\Delta\Phi + c\Phi = e_0 \qquad \text{in } \Omega. \tag{3.12}$$

Assume that the following H^2-regularity holds

$$\|\Phi\|_2 \leq c\|e_0\|. \tag{3.13}$$

Theorem 3.3.2. *Let $u_h \in V_h$ be the SFWG finite element solutions of* (3.4)*. Assume that (3.13) holds true, then there exists a constant C such that*

$$\|e_0\| \leq Ch^4|u|_4. \tag{3.14}$$

Proof. Testing (3.12) by e_0, we have

$$\|e_0\|^2 = (e_0, e_0) = (-\Delta\Phi + c\Phi, e_0).$$

Recall that

$$e_0 = Q_0 u - u_0.$$

By letting $u = \Phi$ and $v_0 = e_0$ in (3.8), we have

$$\|e_0\|^2 = (\nabla_w e_h, \nabla_w Q_h\Phi) + c(\Phi, e_0) - l(\Phi, e_h).$$

Since

$$\begin{aligned}
&(\nabla_w e_h, \nabla_w Q_h\Phi) + c(\Phi, e_0)\\
&= (\nabla_w e_h, \nabla_w Q_h\Phi) + c(Q_0\Phi, e_0)\\
&= l(u, Q_h\Phi),
\end{aligned}$$

we have

$$\begin{aligned}
\|e_0\|^2 &= l(u, Q_h\Phi) - l(\Phi, e_h)\\
&\leq |l(u, Q_h\Phi)| + |l(\Phi, e_h)|.
\end{aligned}$$

We can apply Cauchy-Schwarz inequality to the first term,

$$\begin{aligned}
|l(u, Q_h\Phi)| &= \left| \sum_{T\in\mathcal{T}_h} (Q_0\Phi - Q_b\Phi, \nabla u\cdot\mathbf{n} - \Pi_2\nabla u\cdot\mathbf{n})_{\partial T} \right|\\
&\leq \sum_{T\in\mathcal{T}_h} \|Q_0\Phi - Q_b\Phi\|_{\partial T}\| \|\nabla u\cdot\mathbf{n} - \Pi_2\nabla u\cdot\mathbf{n}\|_{\partial T}.
\end{aligned}$$

By the definition of $Q_h u$, we have below equalities, then we can apply Cauchy-Schwarz inequality

$$\begin{aligned}
\|Q_0\Phi - Q_b\Phi\|_{\partial T}^2 &= (Q_0\Phi - Q_b\Phi, Q_0\Phi - Q_b\Phi)_{\partial T}\\
&= (Q_0\Phi - \Phi, Q_0\Phi - Q_b\Phi)_{\partial T}\\
&\leq \|Q_0\Phi - \Phi\|_{\partial T}\|Q_0\Phi - Q_b\Phi\|_{\partial T}.
\end{aligned}$$

Thus,

$$\|Q_0\Phi - Q_b\Phi\|_{\partial T} \leq \|Q_0\Phi - \Phi\|_{\partial T}.$$

Combining the steps above and applying Cauchy-Schwarz inequality, we have

$$\begin{aligned}|l(u,Q_h\Phi)| &\leq \sum_{T\in\mathcal{T}_h}\|Q_0\Phi-\Phi\|_{\partial T}\|\nabla u\cdot\mathbf{n}-\Pi_2\nabla u\cdot\mathbf{n}\|_{\partial T}\\ &\leq \left(\sum_{T\in\mathcal{T}_h}h_T^{-1}\|Q_0\Phi-\Phi\|_{\partial T}^2\right)^{\frac{1}{2}}\left(\sum_{T\in\mathcal{T}_h}h_T\|\nabla u\cdot\mathbf{n}-\Pi_2\nabla u\cdot\mathbf{n}\|_{\partial T}^2\right)^{\frac{1}{2}}.\end{aligned}$$

Next, by trace inequality (3.10) and interpolation error,

$$\begin{aligned}&\left(\sum_{T\in\mathcal{T}_h}h_T^{-1}\|Q_0\Phi-\Phi\|_{\partial T}^2\right)^{\frac{1}{2}}\\ &\leq\left[\sum_{T\in\mathcal{T}_h}h_T^{-1}(Ch_T^{-1}\|Q_0\Phi-\Phi\|_T^2+Ch_T\|\nabla(Q_0\Phi-\Phi)\|_T^2)\right]^{\frac{1}{2}}\\ &\leq\left[\sum_{T\in\mathcal{T}_h}h_T^{-1}(Ch_T^{-1}(h_T^2|\Phi|_{2,T})^2+Ch_T(h_T|\Phi_{2,T}|)^2)\right]^{\frac{1}{2}}\\ &\leq Ch|\Phi|_{2,\Omega}.\end{aligned}$$

In the proof of (3.9), we have shown that

$$\left(\sum_{T\in\mathcal{T}_h}h_T\|\nabla u\cdot\mathbf{n}-\Pi_2\nabla u\cdot\mathbf{n}\|_{\partial T}^2\right)^{\frac{1}{2}}\leq Ch^3|u|_{4,\Omega}.$$

Thus,

$$|l(u,Q_h\Phi)|\leq Ch^4|\Phi|_2|u|_4\leq Ch^4|u|_4\|e_0\|.$$

We also have, by (3.9) and (3.11) that

$$\begin{aligned}|l(\Phi,e_h)|&\leq Ch|\Phi|_2|||e_h|||\\ &\leq Ch^4|\Phi|_2|u|_4\\ &\leq Ch^4|u|_4\|e_0\|.\end{aligned}$$

Thus $\|e_0\|\leq Ch^4|u|_4$. □

3.4 A Locally Lifted p_3 Solution

In this section, we lift the solution to a P_3 solution to achieve superconvergence. Elementwise, we compute a solution $\hat{u}_h|_T\in P_3(T)$ such that

$$(\nabla\hat{u}_h,\nabla p_3) = (\nabla_w u_h,\nabla p_3),\ \forall p_3\in P_3(T) \tag{3.15}$$

$$(\hat{u}_h,p_0) = (u_0,p_0),\ \forall p_0\in P_0(T). \tag{3.16}$$

Remark 3.4.1. *The square system of equations of (3.15)-(3.16) has an unique solution. When $u_h=0$, $\|\nabla\hat{u}_h\|_0^2=0$, thus $\hat{u}_h$ is a constant. Given (3.16), this constant is zero.*

Theorem 3.4.1. *Let $u\in H_0^1(\Omega)\cap H^4(\Omega)$ be the exact solution of (1.1)-(1.2), let $u_h\in V_h$ be the SFWG finite element solution of (3.4), and let $\hat{u}_h|_T\in P_3(T)$ be locally lifted solution of (3.15)-(3.16). There exists a*

constant C such that

$$\|u - \hat{u}_h\| \leq Ch^4|u|_4. \tag{3.17}$$

Proof. By the definition of L^2 projection and triangle inequality,

$$\|u - \hat{u}_h\| \leq \|\Pi_0(u - \hat{u}_h)\| + \|(I - \Pi_0)(u - \hat{u}_h)\|$$

Applying the definition of L^2 projection multiple times, we have

$$\begin{aligned}
\|\Pi_0(u - \hat{u}_h)\| &= (\Pi_0(u - \hat{u}_h), \Pi_0(u - \hat{u}_h)) \\
&= (u - \Pi_0 u_h, \Pi_0(u - \hat{u}_h)) \\
&= (\Pi_1 u - \Pi_0 u_h, \Pi_0(u - \hat{u}_h)) \\
&= (\Pi_0(\Pi_1 u - h_h), \Pi_0(u - \hat{u}_h)) \\
&= \|\Pi_0(\Pi_1 u - u_h)\|
\end{aligned}$$

Since

$$\|\Pi_0 v\|^2 \leq \|v\|\|\Pi_0 v\|,$$

we have

$$\|\Pi_0(\Pi_1 u - u_h)\| \leq \|\Pi_1 u - u_h\|.$$

Since $\Pi_1 u = Q_0 u$, by (3.14)

$$\|\Pi_1 u - u_h\| \leq Ch^4|u|_4.$$

Thus

$$|\Pi_0(u - \hat{u}_h)\| \leq Ch^4|u|_4.$$

By interpolation error and triangle inequalities, we arrive at the first two inequalities; then we can apply interpolation error to each term separately, we have

$$\begin{aligned}
\|(I - \Pi_0)(u - \hat{u}_h)\| &\leq Ch\|\nabla(u - \hat{u}_h)\| \\
&\leq Ch\|\nabla(u - \Pi_3 u)\| + Ch\|\nabla(\Pi_3 u - \hat{u}_h)\| \\
&\leq Chh^3|u|_4 + Ch\|\nabla(\Pi_3 u - \hat{u}_h)\|.
\end{aligned}$$

Denote $\Pi_3 u - \hat{u}_h$ as w, hence $\nabla w \in [P_2(T)]^2$, and

$$\begin{aligned}
\|\nabla(\Pi_3 u - \hat{u}_h)\|^2 &= (\nabla(\Pi_3 u - \hat{u}_h), \nabla w) \\
&= (\nabla(\Pi_3 u - u), \nabla w) + (\nabla(u - \hat{u}_h), \nabla w)
\end{aligned}$$

By Lemma 3.3.1, (3.15), and Cauchy-Schwarz inequality, we have

$$\begin{aligned}
\|\nabla(\Pi_3 u - \hat{u}_h)\|^2 &= (\nabla(\Pi_3 u - u, \nabla w)) + (\nabla u - \Pi_2(\nabla u), \nabla w) + (\nabla_w Q_h u - \nabla \hat{u}_h, \nabla w) \\
&= (\nabla(\Pi_3 u - u, \nabla w)) + (\nabla u - \Pi_2(\nabla u), \nabla w) + (\nabla_w Q_h u - \nabla_w u_h, \nabla w) \\
&\leq (\|\nabla(\Pi_3 u - u)\| + \|\nabla u - \Pi_2(\nabla u)\| + |||Q_h u - u_h|||)\|\nabla(\Pi_3 u - \hat{u}_h)\|
\end{aligned}$$

By interpolation error and (3.11), the above expression is less than or equal to

$$(Ch^3|u|_4 + Ch^3|u|_4 + Ch^3|u|_4)\|\nabla(\Pi_3 u - \hat{u}_h)\|.$$

Thus, $\|\nabla(\Pi_3 u - \hat{u}_h)\| \leq Ch^3|u|_4$, and $\|(I - \Pi_0)(u - \hat{u}_h)\| \leq Ch^4|u|_4$. Thus, $\|u - \hat{u}_h\| \leq Ch^4|u|_4 + Ch^4|u|_4 = Ch^4|u|_4$. □

3.5 Numerical Experiments

In this section, we examine the stabilizer free WG method by testing its accuracy and convergence order for solving diffusion-reaction equation. For convergence tests, we consider linear base functions for the inside and second order polynomials for the boundary, i.e. $k = 1$. The mesh generation and all computations are conducted in the MATLAB environment; the code can be found in [6].

The main ideas of numerical implementation for two dimension are similar to one dimension but more complicated. We are looking to set up a system of equations, with the unknowns being the coefficients of the base functions. We omit the details, and only present the key ideas behind constructing the stiffness matrix here. Similar to one dimension, we can represent $\nabla_w u$ as a linear combination of the monomials $\mathbf{m}_\alpha(x, y)$, where the monomials are:

$$\{[1,0]^T, [x,0]^T, [y,0]^T, [xy,0]^T, [x^2,0]^T, [y^2,0]^T,$$
$$[0,1]^T, [0,x]^T, [0,y]^T, [0,xy]^T, [0,x^2]^T, [0,y^2]^T\}.$$

Thus we have

$$\nabla_w u(x,y) = \sum_{\alpha=1}^{12} \mathsf{S}^\alpha \mathbf{m}_\alpha(x,y).$$

Following the same idea as in one dimension, we also have: $\mathsf{G}_{i,j} = \int_T \mathbf{m}_i \cdot \mathbf{m}_j dx$. Then

$$(\nabla_w \phi_i(x), \nabla_w \phi_j(x)) = \left(\sum_\alpha \mathsf{S}_i^\alpha \mathbf{m}_\alpha(x), \sum_\alpha \mathsf{S}_i^\alpha m_\alpha(x) \right) = \mathsf{S}_i^T G \mathsf{S}_j.$$

Testing by $\mathbf{m}_\alpha$ and letting $b_i = \mathsf{G}\mathsf{S}_i$, we have

$$(\nabla_w \phi_i, \nabla_w \phi_j) = \mathbf{b_i}^T \mathsf{G}^{-1} \mathbf{b_j}. \tag{3.18}$$

We can compute $\mathbf{b_i}$ by definition:

$$\mathbf{b}_{i,\alpha} = -\int_T \phi_i (\nabla \cdot \mathbf{m}_\alpha) d\mathbf{x}.$$

For example,

$$\mathbf{b}_{1,5} = -\int_T \phi_i (\nabla \cdot \mathbf{m}_5) d\mathbf{x} = -\int_T 2\phi_i x d\mathbf{x}.$$

We can then use Gaussian quadrature in two dimensions to calculate $-\int_T 2\phi_i x d\mathbf{x}$, then assemble the components to calculate $(\nabla_w \phi_i, \nabla_w \phi_j)$.

3.5.1 Example 1: Trigonometric solution over a squared domain

We solve the following diffusion-reaction equation on the unit square $[0,1] \times [0,1]$:

$$-\Delta u + u = 2\pi^2 \sin(\pi x)\sin(\pi y) + \sin(\pi x)\sin \pi y.$$
$$u(x,y) = 0 \text{ on } \partial\Omega$$

The exact solution is

$$u(x,y) = \sin(\pi x)\sin(\pi y) \tag{3.19}$$

The first level triangular mesh consists of two unit right triangles cutting from the unit square by a backward slash. We present the third level uniform triangular mesh used in this experiment in Figure 3.1. The high level grids are the half-size refinements of the previous grid.

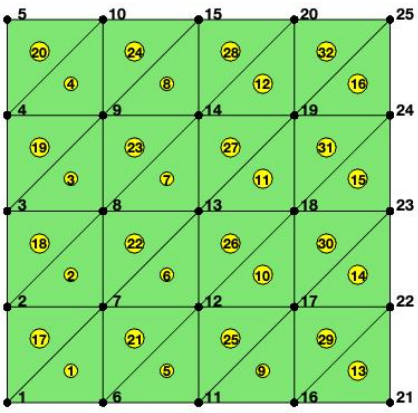

Figure 3.1: Example of mesh construction for squared two dimension

The error and the order of convergence are shown in Table 3.1. We are expecting order 3 convergence and order 4 convergence for the energy norm and L^2 norm, respectively. The numerical results confirm the convergence theory.

In Figure 3.2, we plot the finite element solution on second, fourth, and fifth level triangular grid. We can see, the solutions are more and more accurate as the mesh size decrease.

Table 3.1: Error profiles and convergence rates for solution (3.19)

Grid	$\|\Pi_1 u - u_0\|$	rate	$\|\|\|Q_h u - u_h\|\|\|$	rate
2	$7.9283e-04$	4	$1.1023e-02$	3
3	$5.2668e-05$	4	$1.4316e-03$	3
4	$3.3471e-06$	4	$1.8134e-04$	3
5	$2.1014e-07$	4	$2.2781e-05$	3
6	$1.3150e-08$	4	$2.8535e-06$	3

3.5.2 Example 2:Trigonometric solution over L-shaped domain

We solve the following diffusion-reaction equation on the L-shaped domain $[-1,1]\times[-1,1]\backslash[0,1]\times[0,1]$:

$$-\Delta u + u = 2\pi^2 \sin(\pi x)\sin(\pi y) + \sin(\pi x)\sin \pi y.$$
$$u(x,y) = 0 \text{ on } \partial\Omega$$

The exact solution is

$$u(x,y) = \sin(\pi x)\sin(\pi y). \tag{3.20}$$

Unlike the previous example, for this example, we use unstructured mesh and Delaunay triangulation to construct the triangles.

The error and the order of convergence are shown in Table 3.2. We are expecting order 3 convergence and order 4 convergence for the energy norm and L^2 norm, respectively. The numerical results confirm the convergence theory.

Table 3.2: Error profiles and convergence rates for solution (3.20)

Grid	$\|\Pi_1 u - u_0\|$	rate	$\|\|\|Q_h u - u_h\|\|\|$	rate
2	$1.4761e-04$	4	$4.0319e-03$	3
3	$9.6409e-06$	4	$5.0853e-04$	3
4	$6.1074e-07$	4	$6.3655e-05$	3
5	$3.8328e-08$	4	$7.9602e-06$	3

In Figure 3.3 , we plot the finite element solution on the third level triangular grid to give a general sense of the domain, numerical solution, and the triangulation.

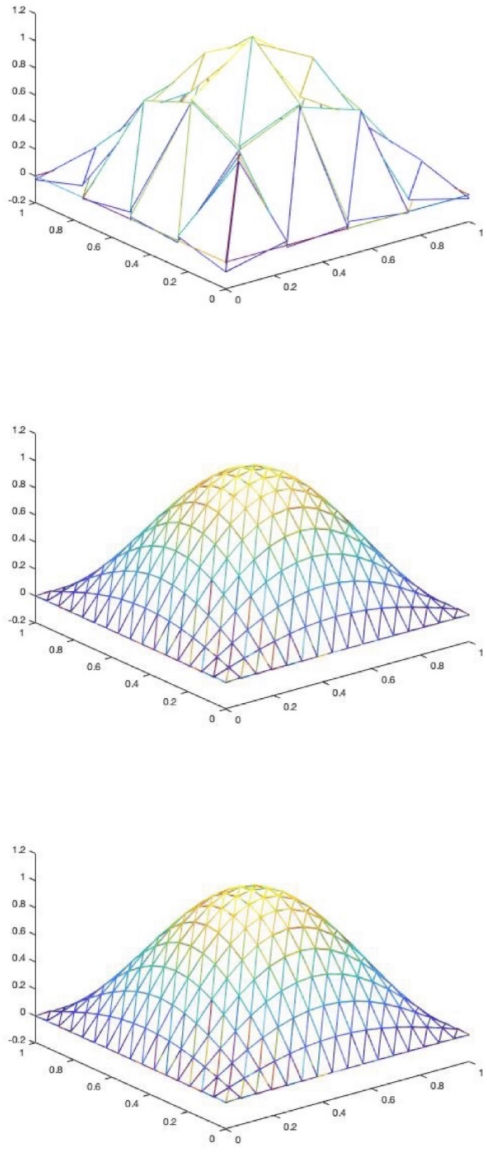

Figure 3.2: Finite Element Solution on Second, Fourth, and Fifth Level Triangular Grid

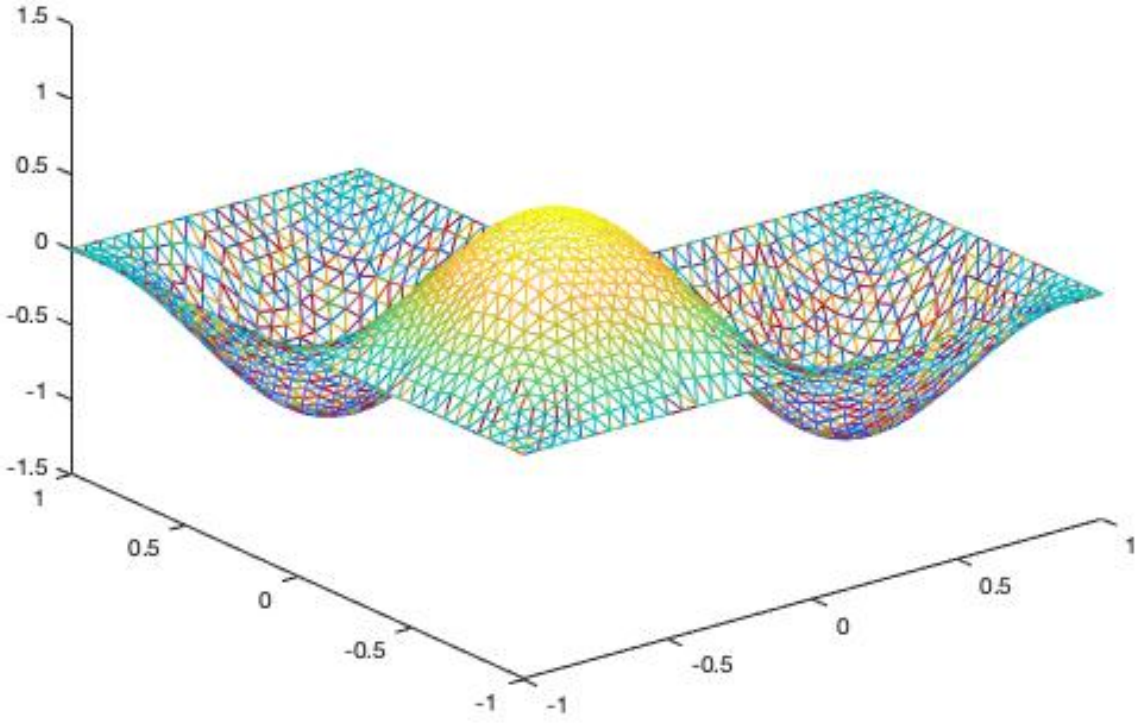

Figure 3.3: Finite Element Solution on Third Level Grid for Solution (3.20)

Chapter 4

Conclusion and future work

In this thesis, we applied SFWG to the diffusion reaction equation and proved that it achieves superconvergence of order 3 for energy norm and order 4 for L^2 norm. We used linear basis functions for one dimensional case and applied linear basis functions for the interior and quadratic basis for the edges for the two dimensional case. We conducted numerical experiments to validate the results.

Ye and Zhang [15] apply the SFWG method to the Poisson equation in one dimension. This work utilizes the same method, but extends these results in two different ways. First, we work with the reaction diffusion equation; setting the reaction term to zero recovers the Poisson equation. Second, we discuss both one and two dimensions.

Since the coefficient of our reaction term was set to be positive, the theoretical part was not too hard to complete.However, in the numerical implementation, the mass matrix needed to be computed in order to match the reaction term. As for the numerical implementation for the one dimensional case, we experienced the most difficulty during the programming of code for the lifted solution. The code we developed for the one dimensional case only applies to zero boundary conditions; further modification can be done to allow the possibility for various boundary conditions.

For the two dimensional case, even though we proved the superconvergence of the lifted solution, it was not easy not design an computational algorithm to get the related numerical results. The work for this will be done in the near future.

More future works on SFWG may involve the possibility of extending this work to higher dimension, employing higher degree basis functions and observing their performance, and applying the method to more partial differential equations and examining the performance of the scheme.

Bibliography

[1] Zhiqiang Cai and Seokchan Kim. "A Finite Element Method Using Singular Functions for the Poisson Equation: Corner Singularities". In: *SIAM Journal on Numerical Analysis* 39.1 (2001), pp. 286–299. DOI: 10.1137/S0036142999355945. eprint: https://doi.org/10.1137/S0036142999355945. URL: https://doi.org/10.1137/S0036142999355945.

[2] Long Chen. *iFEM: an integrated finite element methods package in MATLAB*. Tech. rep. 2009. URL: https://github.com/lyc102/ifem.

[3] Gouri Dhatt, Emmanuel Lefrançois, and Gilbert Touzot. *Finite element method*. John Wiley & Sons, 2012.

[4] Robert Eymard, Thierry GallouÃ«t, and RaphaÃšle Herbin. "Finite volume methods". In: *Solution of Equation in ân (Part 3), Techniques of Scientific Computing (Part 3)*. Vol. 7. Handbook of Numerical Analysis. Elsevier, 2000, pp. 713–1018. DOI: https://doi.org/10.1016/S1570-8659(00)07005-8. URL: https://www.sciencedirect.com/science/article/pii/S1570865900070058.

[5] Juan Gutierrez, Ming-Jun Lai, and George Slavov. "Bivariate Spline Solution of Time Dependent Nonlinear PDE for a Population Density over Irregular Domains". In: *Mathematical biosciences* 270 (Sept. 2015). DOI: 10.1016/j.mbs.2015.08.013.

[6] *Implementation of Weak Galerkin Finite Element Methods*. Computer program. 2016. URL: https://github.com/MollyRaver/WGFEMPoisson.

[7] Christina Kuttler. "Reaction-diffusion equations with applications". In: *Internet seminar*. 2011.

[8] Lin Mu, Junping Wang, and Xiu Ye. *Weak Galerkin Finite Element Methods for the Biharmonic Equation on Polytopal Meshes*. 2013. DOI: 10.48550/ARXIV.1303.0927. URL: https://arxiv.org/abs/1303.0927.

[9] Lin Mu, Junping Wang, and Xiu Ye. "A weak Galerkin finite element method with polynomial reduction". In: *Journal of Computational and Applied Mathematics* 285 (2015), pp. 45–58. ISSN: 0377-0427. DOI: https://doi.org/10.1016/j.cam.2015.02.001. URL: https://www.sciencedirect.com/science/article/pii/S037704271500059X.

[10] Gordon D Smith, Gordon D Smith, and Gordon Dennis Smith Smith. *Numerical solution of partial differential equations: finite difference methods*. Oxford university press, 1985.

[11] Ahmed Al-Taweel and Xiaoshen Wang. "A note on the optimal degree of the weak gradient of the stabilizer free weak Galerkin finite element method". In: *Applied Numerical Mathematics* 150 (2020), pp. 444–451.

[12] Junping Wang and Xiu Ye. "A Weak Galerkin Finite Element Method for Second-Order Elliptic Problems". In: (2011). DOI: 10.48550/ARXIV.1104.2897. URL: https://arxiv.org/abs/1104.2897.

[13] Greg von Winckel. *Legende-Gauss-Radau Nodes and Weights*. file. 2004. URL: https://www.mathworks.com/matlabcentral/profile/authors/869721.

[14] Xiu Ye and Shangyou Zhang. *On stabilizer-free weak Galerkin finite element methods on polytopal meshes*. 2019. DOI: 10.48550/ARXIV.1906.06634. URL: https://arxiv.org/abs/1906.06634.

[15] Xiu Ye and Shangyou Zhang. *Achieving superconvergence by one dimensional discontinuous finite elements. Part I. The WG Method*. Preprint. 2021. URL: https://drive.google.com/file/d/1hcRHFaNqHWBZNPsNSIAqmGR8phY9DXLT/view.